

## BIROn - Birkbeck Institutional Research Online

Chen, B. and Li, S. and Pogge von Strandmann, Philip A.E. and Sun, J. and Zhong, J. and Li, C. and Ma, T. and Xu, S. and Liu, C. (2019) Ca isotope constraints on chemical weathering processes: evidence from headwater in the Changjiang River, China. *Chemical Geology* 531 , p. 119341. ISSN 0009-2541.

Downloaded from: <https://eprints.bbk.ac.uk/id/eprint/30038/>

*Usage Guidelines:*

Please refer to usage guidelines at <https://eprints.bbk.ac.uk/policies.html>  
contact [lib-eprints@bbk.ac.uk](mailto:lib-eprints@bbk.ac.uk).

or alternatively

1 **Ca isotope constraints on chemical weathering processes:**

2 **Evidence from headwater in the Changjiang River, China**

3  
4 **Bei-Bei Chen <sup>a</sup>, Si-Liang Li <sup>a, b, \*</sup>, Philip A.E. Pogge von Strandmann <sup>c</sup>,**  
5 **Jian Sun <sup>d</sup>, Jun Zhong <sup>a</sup>, Cai Li <sup>a</sup>, Ting-Ting Ma <sup>a</sup>, Sen Xu <sup>a</sup>, Cong-Qiang**  
6 **Liu <sup>a</sup>**

7  
8 *a* Institute of Surface-Earth System Science, Tianjin University, Tianjin 300072,  
9 China

10 *b* State Key Laboratory of Hydraulic Engineering Simulation and Safety, Tianjin  
11 University, Tianjin 300072, China

12 *c* London Geochemistry and Isotope Centre (LOGIC), Institute of Earth and  
13 Planetary Sciences, University College London and Birkbeck, University of  
14 London, Gower Street, London WC1E 6BT, UK

15 *d* Key Laboratory of Deep-Earth Dynamics of Ministry of Natural Resources,  
16 MNR Key Laboratory of Isotope Geology, Institute of Geology, Chinese  
17 Academy of Geological Sciences, Beijing 100037, China

18  
19 **Manuscript submitted to *Chemical Geology* (14-June-2019)**

20 \*Corresponding authors: Si-Liang Li

21 State Key Laboratory of Hydraulic Engineering Simulation and Safety,

22 Tianjin University 92# Wei-Jin Road, Nankai District

23 Tianjin 300072, China

24 Fax: (+86-22) 8737 0955

25 Email: Siliang.li@tju.edu.cn

## Abstract

This study aims to clarify the relationship between chemical weathering of rocks and the carbon budget of rivers and to better understand the weathering mechanisms of plateau watersheds. We chose to study the Jinsha River, which originates from the Tibetan Plateau and also is in the upper reaches of the Changjiang River. Analysis of hydrochemistry, radiogenic strontium isotope and stable calcium isotopes were conducted of the Jinsha River water samples, which were collected along its mainstream and main tributaries in the summer. The results show that the water chemistry of the mainstream is dominated by evaporite weathering, which has a low  $^{87}\text{Sr}/^{86}\text{Sr}$  (0.7098 to 0.7108) and wide range of Sr contents (2.70 to 9.35  $\mu\text{mol/L}$ ). In contrast, tributaries of the Jinsha River have higher  $^{87}\text{Sr}/^{86}\text{Sr}$  (0.7090 to 0.7157) and lower Sr contents ( $\sim 1 \mu\text{mol/L}$ ). Moreover, the Ca isotopic compositions in the mainstream (0.87-1.11‰) are heavier than the tributaries (0.68-0.88‰) and could not attribute to the conventional mixing of different sources. We suggest that secondary carbonate precipitation fractionates Ca isotopes in the Jinsha River, and fractionation factors are between 0.99935 and 0.99963. At least 66% of dissolved Ca is removed in the mainstream of the Jinsha River through secondary mineral precipitation, and the average value is  $\sim 35\%$  in the tributaries. The results highlight that evaporite weathering results in more carbonate precipitation influencing Ca transportation and cycling in the riverine system constrained by stable Ca isotopic compositions and water chemistry.

**Key words:** Ca isotopes, Chemical weathering, Secondary carbonate precipitation, Isotope fractionation.

## 1. Introduction

Calcium is the fifth most abundant element in the earth's crust and can migrate easily between major geochemical reservoirs at the Earth's surface ([Rudnick and Gao, 2014](#); [Tipper et al., 2016](#)). As one of major components of rock and minerals, Ca is participant in many critical processes related to the co-evolution of earth and life, including carbon cycling, the evolution of marine chemical components and long-term climate change ([Berner and Berner, 2012](#); [Berner, 2003](#); [Berner et al., 1983](#); [Walker et al., 1981](#)). Chemical weathering of rocks and minerals plays a key role in those processes, in which rocks and minerals react with dissolved acidic gases (such as CO<sub>2</sub> and SO<sub>2</sub>) and water in the atmosphere, releasing dissolved metal ions and forming secondary minerals. Solutes are transported to the ocean through rivers, regulating the chemical balance of seawater and absorbing CO<sub>2</sub> in the atmosphere to bury them in the form of carbonate ([Gaillardet et al., 1999](#); [Schmitt et al., 2003](#); [West et al., 2005](#); [White and Blum, 1995](#)). Other products of rock weathering, such as clay minerals, will be accumulated to the floodplain along the river, forming an important part of soil ([Tipper et al., 2006](#); [Torres et al., 2015](#); [West et al., 2005](#)).

Riverine input of Ca is a key component in the global Ca model, where

oceans impact climate through regulation of atmospheric CO<sub>2</sub> ([Gaillardet et al., 1999](#)). The study of Ca fluxes and their isotopic compositions in rivers could help understand whether Ca in the ocean is in equilibrium ([DePaolo, 2004](#); [Schmitt et al., 2003](#); [Tipper et al., 2010](#); [Zhu and Macdougall, 1988](#)). This also determines whether the Ca isotopes can be used as an indicator for the study of the paleo-ocean to explore paleo-sea surface temperature (SST) and its corresponding P<sub>CO2</sub>, which are closely related to long-term climate change ([DePaolo, 2004](#); [Fantle, 2010, 2015](#); [Fantle and DePaolo, 2005](#); [Pogge von Strandmann et al., 2013](#); [Pogge von Strandmann et al., 2012](#); [Rocha and DePaolo, 2000](#)). On the other hand, riverine Ca fluxes produced by rock weathering are an important part of the ocean Ca budget, which has a significant impact on the global carbon cycle together with the precipitation of carbonate in the ocean ([Schmitt, 2016](#); [Tipper et al., 2016](#)). Many studies have focused on the behavior of Ca isotopes during rock weathering and material transport by rivers ([Cenki-Tok et al., 2009](#); [Fantle and Tipper, 2014](#); [Hindshaw et al., 2013](#); [Hindshaw et al., 2011](#); [Jacobson et al., 2015](#); [Lehn et al., 2017](#); [Marie-Laure Bagard et al., 2013](#); [Marie-Laure Bagard et al., 2011](#); [Moore et al., 2013](#); [Schmitt, 2016](#); [Schmitt et al., 2003](#); [Tipper et al., 2006](#); [Tipper et al., 2010](#); [Tipper et al., 2008](#); [Tipper et al., 2016](#); [Wiegand and Schwendenmann, 2013](#)). Ca isotopes could not only trace the Ca cycle directly but also be a potential tracer in mineral carbonation and the C cycle ([Pogge von Strandmann et al., 2019a](#)).

Previous studies show that Ca isotopes in rivers may mainly controlled by different factors across different scales. For small rivers, a variety of factors result in changeable Ca isotopic compositions ( $\delta^{44/40}\text{Ca}$ ) which exhibit a wide range from 0.27 to 1.70‰. Ca isotopic compositions are not only controlled by mixing of different sources, such as lithology, underground water and soil water ([Hindshaw et al., 2011](#); [Jacobson et al., 2015](#); [Jacobson and Holmden, 2008](#); [Jacobson and Wasserburg, 2005](#)), but also by secondary processes, such as the uptake of plants ([Brazier et al., 2019](#); [Cenki-Tok et al., 2009](#); [Farkaš et al., 2011](#); [Hindshaw et al., 2012](#); [Holmden and Bélanger, 2010](#); [Schmitt et al., 2017](#)), the neoformation of secondary mineral phases (soil carbonates, travertines and Ca-bearing clays) ([Hindshaw et al., 2013](#); [Tipper et al., 2006](#)) and the adsorption by clays ([Brazier et al., 2019](#); [Ockert et al., 2013](#)). With regards to world rivers, although complex lithology and variable climate and vegetations result in different hydrochemistry and Sr isotopic compositions, the ratios of Ca isotopes are quite homogeneous ([Schmitt, 2016](#)). Samples collected at river mouths show small  $\delta^{44/40}\text{Ca}$  variations of 0.56‰, ranging from 0.69 to 1.25‰ with an average of 0.86‰ ([Schmitt et al., 2003](#); [Tipper et al., 2010](#); [Zhu and Macdougall, 1988](#)). The main controlling factors of Ca isotopes in world rivers are still controversial. Fantle and Tipper ([2014](#)) calculated the average Ca isotopic composition of carbonate and silicate as 0.6‰ and 0.94‰ respectively. Combined with the global riverine Ca flux, the mean theoretical Ca isotope ratio of the riverine flux is 0.63 to 0.69‰, which is lower than the measured value of

continental runoff ( $0.86 \pm 0.06\text{‰}$ ) ([Tipper et al., 2016](#)). Therefore, they suggested that secondary processes, such as the plant uptake, secondary mineral formation and clay adsorption, play an important role in the riverine Ca isotopic composition. However, Jacobson et al. ([2015](#)) analyzed riverine Ca isotope values in Iceland, and demonstrated that the dissolution of hydrothermal calcite in basalt dominates the Ca isotopic ratios of river in Iceland. They also suggested that conventional mixing processes stemming from mineral dissolution dominates the Ca isotopic compositions of global rivers. These studies suggested riverine Ca behavior relating with geological characteristics were not well explored and the dominant factors controlling riverine Ca isotopes still need to be further clarified.

Overall, the monitoring of Ca isotope behavior along rivers is still lacking ([Schmitt et al., 2003](#); [Tipper et al., 2010](#); [Zhu and Macdougall, 1988](#)). Although the factors affecting the Ca isotope value of rivers can be evaluated qualitatively, some critical isotope signals may be overprinted ([Hindshaw et al., 2013](#)), meaning that it is difficult to fully understand and interpret Ca isotope ratios.

Moreover, abundant previous studies focus on silicate weathering ([Cenki-Tok et al., 2009](#); [Hindshaw et al., 2013](#); [Hindshaw et al., 2011](#); [Holmden and Bélanger, 2010](#); [Marie-Laure Bagard et al., 2013](#); [Nielsen and DePaolo, 2013](#); [Schmitt et al., 2003](#); [Wiegand and Schwendenmann, 2013](#)), and several researchers have studied the effect of sedimentary rocks weathering on carbon budget ([Gaillardet et al., 2018](#); [Lehn et al., 2017](#); [Moore et al., 2013](#); [Tipper et](#)

al., 2006; [Tipper et al., 2008](#)), but studies on evaporite weathering are very rare ([Wang et al., 2018](#); [Wellman and Wilson, 1965](#)). As a common rock in the earth-surface, evaporites are often accompanied by sedimentary rocks, such as limestone, dolomite and mudstone. Although the total amount of evaporites is less than that of silicates and carbonates, it has great influence on water chemistry owing to its high solubility and fast dissolution rate ([Wang et al., 2018](#); [Wellman and Wilson, 1965](#)). For example, the dissolution of gypsum releases a large amount of Ca into the water, which to a certain extent increases the absorption of CO<sub>2</sub> by the river and affects the overall carbon budget ([Farkaš et al., 2007](#)). Previous studies on the Ca isotopes of evaporites have been focused on evaporites from seafloor hydrothermal precipitation ([Amini et al., 2008](#); [Blättler and Higgins, 2014](#); [Galy and France-Lanord, 1999](#); [Hensley, 2006](#); [Holmden, 2009](#)) and several laboratory precipitation experiments of anhydrite ([Harouaka et al., 2014](#); [Hensley, 2006](#); [Lemarchand et al., 2004](#)), which were used to assess the impact of seafloor hydrothermal input on marine Ca isotopic compositions. However, evaluations of the influence of continental evaporite weathering on water chemistry and even Carbon budget are still rare ([Jacobson and Holmden, 2008](#); [Jacobson and Wasserburg, 2005](#); [Russell et al., 1978](#)).

In this study, we collected water samples from the mainstream and main tributaries of the upper Jinsha River. Water chemistry in the mainstream is mainly dominated by evaporates dissolution ([Chetelat et al., 2008](#); [Gaillardet et al., 1999](#); [Noh et al., 2009](#); [Wu et al., 2008](#); [Zhao et al., 2019](#); [Zhong, 2017](#)).



Through analyzing data of hydrochemistry, Ca and Sr isotopes in the Jinsha River Basin, the dominant factors controlling the calcium transportation of the Jinsha River are evaluated, then the influence of evaporite weathering on carbon transportation is assessed, which could lay a foundation for further exploring the mechanism of solute transportation impacted by secondary processes in the rivers origin from the Tibetan Plateau.

## 2. Regional setting

The Jinsha River Basin is located in the eastern Tibetan Plateau, Southwest China. As the headwaters of the Changjiang River, the Jinsha River originates at the end of the ice tongue of the Gladandong Mountains in the middle of the Tanggula Mountains in Qinghai Province at an elevation of 6621 m. The source river of the Changjiang River is mainly composed of Dangqu (south source), Tuotuo River (the main source) and Chumar River (north source). They converge as the Tongtian River, which flowed southeast to accept the Batang River near Yushu County, Qinghai Province, after which it is called the Jinsha River ([Su and Chen, 2016](#); [Wu et al., 2011](#); [Wu et al., 2009a](#); [Wu et al., 2008](#); [Zhang et al., 2016](#); [Zhao et al., 2019](#)) (Fig. 1a). The Jinsha River has a basin area of 473,640 km<sup>2</sup> with a mainstream river length of over 2316 km, accounting for 2/3 of the length of the upper reaches of the Changjiang River ([Su and Chen, 2016](#)). The upper, middle, and lower reaches of the river are divided by Shigu and Panzhihua stations. Significant differences in topography

and geomorphology are observed in the Jinsha River Basin, leading to great differences in regional climate and water cycle processes in the upper, middle and lower reaches ([Xie et al., 2018](#)). The source region of the Jinsha River is located in the southeast of the Qinghai-Tibet Plateau, with an average altitude of more than 5000 m, showing typical plateau landscape where climate is cold and dry. Runoff of source river is mainly supplied by ice and snow melt water and permafrost, so that water cycle is significantly affected by air temperature. The upper reach of the Jinsha River is accompanied by significant topographic differences changing from plateau to typical dry-hot valley. Surrounded by mountains, external water vapor rarely enters, leading to rare precipitation and significant evaporation. The middle reaches of the Jinsha River flow between the deep canyons. The average annual precipitation increases from northwest to southeast, mostly ranging from 600 mm to 1000 mm, and reaches 1300mm in some areas. As to the lower reach of the Jinsha River, terrain changes from canyon to hilly and plain. The average annual precipitation is 600 - 1500 mm and in some areas more than 1800 mm, and the evaporation is small. The water cycle in this area is different from that in the upper and middle reaches on account of the great influence of human activity ([Liu, 2016](#); [Lu et al., 2016](#); [Xie et al., 2018](#); [Zhang et al., 2016](#); [Zhang et al., 2018](#)).

The upper and middle reaches of the Jinsha River were selected as our research area because of little anthropogenic impact ([Zhao et al., 2019](#)) (Fig. 1). Evaporites weathering significantly affect the Jinsha River mainstream

([Chetelat et al., 2008](#); [Gaillardet et al., 1999](#); [Noh et al., 2009](#); [Zhao et al., 2019](#); [Zhong, 2017](#)). Mesozoic clastic rocks and evaporites are mainly exposed in the source area, and the research area in this study is mainly composed of Triassic low-grade metamorphic rocks, Paleozoic carbonate rocks and basalts, accompanied with scattered Mesozoic granitoids and Mesozoic ophiolitic mélanges along the upper reach valley ([Wu et al., 2009a](#); [Wu et al., 2008](#); [Wu et al., 2013](#); [Zhang et al., 2016](#); [Zhao et al., 2019](#)).

### **3. Method**

#### **3.1 Water samples**

Water samples were collected in June 2016, corresponding to the high flow season. Temperature, electrical conductivity and pH of the water samples were measured in the field. Alkalinity was determined by HCl titration. Water samples were filtered through 0.45 µm cellulose-acetate filters into a series of pre-cleaned HDPE bottles for analysis. Major cations (Ca, Mg, Na, K) and Si concentrations were measured by ICP-OES with a precision better than 5% (2 $\sigma_{\text{mean}}$ ). Anions (Cl, SO<sub>4</sub>) were determined by ionic chromatography Dionex 90 with a precision of 5%. The values of partial pressure of CO<sub>2</sub> (P<sub>CO2</sub>) and calcite saturation index (CSI) were calculated by the programmer PhreeqC ([Parkhurst and Appelo, 1999](#)).

### 3.2 Sample preparation for isotopic analysis

Both Ca and Sr are recovered together from the AG50 X12 columns. Because Ca is isotopically fractionated by this resin, quantitative recovery is necessary. River samples were dried down and re-dissolved in 1ml ultrapure HNO<sub>3</sub> on a hot plate at 120°C for 24 h. They were then dried and cooled down to room temperature, and then re-dissolved in 1ml ultrapure HNO<sub>3</sub> with 100 µL H<sub>2</sub>O<sub>2</sub> on a hot plate at 90°C for 1 h to remove organic matter. Note that then these samples also need to be dried down no higher than 90°C to prevent H<sub>2</sub>O<sub>2</sub> from exploding when heated. After that, they were re-dissolved in 1 ml ultrapure HCl for 1 h and then dried down at 120°C. They were finally dried and re-dissolved in 1ml 2N HCl for chemical purification.

The protocols for Ca and Sr separation in this study are modified from ([Chu et al., 2006](#); [Nan et al., 2015](#); [Owen et al., 2016](#)). The column used a 30mL Teflon® micro-column with 6.4mm ID × 9.6mm OD (Savillex®), filled with 2mL AG50W-X12 resin (200-400 mesh, Bio-Rad, USA). Columns were precleaned with 20mL 6 mol/L HNO<sub>3</sub> and 3mL 6 mol/L HCl, and then conditioned with 3mL 18.2 MΩ H<sub>2</sub>O, before sample loading.

1mL sample solutions containing ~100ug Ca were loaded and 19mL 2 mol/L HCl was used to elute the matrix elements including Na, Mg, K, Fe and Mn. Ca was then collected with 18mL 2 mol/L HCl. Following Ca collection, 2mL 3 mol/L HCl was used to elute the tailing of trace Ca. Sr was then collected with 10mL 3 mol/L HCl. Both 2mL aliquots before and after the Ca-cut were collected

and measured for their Ca contents to test whether the Ca elution curve drifted during the chromatographic process. After the column protocols, Ca and Sr collections were dried and dissolved in concentrated HNO<sub>3</sub>, evaporated to dryness three times, and finally dissolved in 0.3 mol/L HNO<sub>3</sub> before isotope analysis ([Sun et al., 2019](#)).

Ca isotopic analysis was undertaken using the Nu Instruments MC-ICPMS at the Laboratory of Isotope Geology, Institute of Geology, Chinese Academy of Geological Sciences, Beijing, China. Isotopes of <sup>42</sup>Ca, <sup>43</sup>Ca and <sup>44</sup>Ca were measured at low-resolution. The standard-sample bracketing (SSB) approach ([Belshaw et al., 2000](#)) was used to correct the mass discrimination, using NIST 915a or NIST 915b as the reference standard, and with sample and standard solutions being matched to give <sup>42</sup>Ca intensities with differences less than 10%. All samples were normally repeatedly analyzed for 3~5 times for one session. The external precision of Ca isotope ratios (<sup>44</sup>Ca/<sup>42</sup>Ca) during the measuring period is better than 0.07‰ (2SD) based on the repeated measurements of standard NIST 915b. Calcium isotope values can be converted using:

$$\delta^{44/40}\text{Ca} = 2.048 \times \delta^{44/42}\text{Ca} \quad (\text{Heuser et al., 2016}). \quad (1)$$

Data in this study are presented as  $\delta^{44/40}\text{Ca}$  relative to the NIST SRM915a standard:

$$\delta^{44/40}\text{Ca} (\text{‰}) = 1000 \left\{ \frac{\left( ^{44}\text{Ca}/^{40}\text{Ca} \right)_{\text{sample}}}{\left( ^{44}\text{Ca}/^{40}\text{Ca} \right)_{\text{SRM 915a}}} - 1 \right\} \quad (2)$$

Sr isotopic analysis was undertaken at the Institute of Surface-Earth

System Science, Tianjin University. The Sr isotope composition were measured using MC-ICPMS and the instrumental mass fractionation was corrected by internally normalizing the  $^{87}\text{Sr}/^{86}\text{Sr}$  ratio to 0.1194. The average  $^{87}\text{Sr}/^{86}\text{Sr}$  ratio for NBS 987 was  $0.710271 \pm 0.000030$  (2SD, n = 34).

## 4. Results

### 4.1 Water chemistry

The pH of the river water samples ranges from 8.06 to 8.66 with an average of 8.35 (Table 1). The temperature of river water is 12.7 to 22.4°C with an average of 16.3°C. The chemical compositions for the Jinsha River waters vary significantly (Chetelat et al., 2008; Gaillardet et al., 1999; Noh et al., 2009; Wu et al., 2008; Zhao et al., 2019; Zhong, 2017), with the total dissolved solids (TDS = Ca + Mg + Na + K + Cl + HCO<sub>3</sub> + SO<sub>4</sub> + SiO<sub>2</sub>) ranging from 88 to 689 mg/L. The range of TDS values in the mainstream (301~689 mg/L) is higher than tributaries' values (88~268 mg/L), and decrease from the upper reach to the lower reach. The total cationic charges ( $\text{TZ}^+ = 2 \times \text{Ca} + 2 \times \text{Mg} + \text{Na} + \text{K}$ ) vary dramatically ranging from 1130  $\mu\text{eq/L}$  to 10,120  $\mu\text{eq/L}$ . Ca<sup>2+</sup> and Mg<sup>2+</sup> are the dominant cations in tributaries accounting for 59-96% of the total cationic budget. In the mainstream, Na<sup>+</sup> is the dominant cation, accounting for 37-56% for the total cationic budget. Besides, the dominant anions are HCO<sub>3</sub><sup>-</sup> and Cl<sup>-</sup> in the main river water. Cl<sup>-</sup> value of the mainstream samples gradually decrease from upstream to downstream, HCO<sub>3</sub><sup>-</sup> in tributaries show large variations and is

the dominant anion. Ca/Na ratios of the main river ranging from 0.24 to 0.59, which are lower than that of tributaries ranging from 4.50 to 11.39. Similarly, the range of Mg/Na ratios of mainstream is from 0.16 to 0.29 while that of tributaries is from 1.61 to 3.54.

In addition, to evaluate the calcite saturation state for river waters, calcite saturation indices (CSI) were calculated based on alkalinity, pH, temperature and ionic strength using the PHREEQC program ([Parkhurst and Appelo, 1999](#)). Results show that nearly all the Jinsha river waters are supersaturated for calcite ([Table 2](#)).

## 4.2 Strontium and its isotopic composition in the Jinsha River

The  $^{87}\text{Sr}/^{86}\text{Sr}$  ratios and Sr concentrations of waters from the Jinsha River Basin are given in [Table 1](#). The range of  $^{87}\text{Sr}/^{86}\text{Sr}$  in the mainstream is similar to source rivers ([Fig. 2](#)) ([Noh et al., 2009](#); [Wu et al., 2009a](#); [Zhao et al., 2003](#)). Moreover, the median value of the source rivers is similar to that of the main stream and tributaries of the Jinsha River, which are close to 0.7100. However, the  $^{87}\text{Sr}/^{86}\text{Sr}$  range of the Jinsha River sediments (JS sediment) is 0.7110 - 0.7147 ([Wu et al., 2009b](#)), which is higher than that of the source area, the tributaries and mainstream of the Jinsha River.

The mainstream of the Jinsha River (JS mainstream) has low variation in  $^{87}\text{Sr}/^{86}\text{Sr}$  ratios with a narrow range of 0.7098 to 0.7108 and an average value of 0.7105, but shows significant changes in Sr contents from 2.70  $\mu\text{mol/L}$  to

9.35  $\mu\text{mol/L}$  with a general decrease from the upper reach to lower reaches (Table 1, Fig. 3a). However, Sr contents of tributaries are almost constant ( $\sim 1\mu\text{mol/L}$ ).  $^{87}\text{Sr}/^{86}\text{Sr}$  ratios of the tributaries have a wider range, from 0.7090 to 0.7157 with an average of 0.7121 (Table 1; Fig. 3a).

Moreover,  $1/\text{Sr}$  shows the strong positive correlation with  $\text{Si}/\text{TZ}^+$  (Fig. 3b), which implies a trend of mixing endmembers. Low  $1/\text{Sr}$  and  $\text{Si}/\text{TZ}^+$  signatures in the waters could be related to carbonate and/or evaporite weathering in the Jinsha River Basin. Moreover, silicate weathering will lead to high  $1/\text{Sr}$  and  $\text{Si}/\text{TZ}^+$  signature in the waters. While the main stream also shows a simple mixing relationship when plotting Sr isotopes against  $1/\text{Sr}$ , the tributaries do not have such a clear relationship (Fig. 3a), suggesting additional endmember contributions.

#### 4.3 Ca isotopic compositions of the Jinsha River waters and gypsums

The  $\delta^{44/40}\text{Ca}$  of the dissolved load in the Jinsha River ranges from 0.68‰ to 1.11‰ with an average of 0.87‰, within the range of other large global rivers (0.42-1.62 ‰) (Schmitt et al., 2003; Tipper et al., 2006; Zhu and Macdougall, 1988).

The highest  $\delta^{44/40}\text{Ca}$  value (1.11‰) is observed in the upstream reach of the main stream (JS-1) and the lowest value (0.68‰) in a tributary in the upper reach (JS-9). There is no systematic change trend of  $\delta^{44/40}\text{Ca}$  from upstream to downstream. In general, the mainstream generally has a higher  $\delta^{44/40}\text{Ca}$



than the tributaries. Furthermore,  $\delta^{44/40}\text{Ca}$  values have a significant positive relationship with  $\text{SO}_4/\text{Ca}$  (Fig. 4a), and a slight negative correlation with  $\text{Si}/\text{Ca}$  (Fig. 4b).

Moreover, rivers draining different lithological sources show a considerable spread in Ca isotopic compositions based on literature compilations of data (Fig. 5). As a regional river originating from the Tibetan Plateau, the Jinsha River has the same Ca isotopic range as rivers from the High Himalayan Crystalline Series (HHCS) (0.69-0.92‰), which is lower than some Ca isotopic values in rivers draining dolostone from Lesser Himalayan Series (LHS) (0.99-1.41‰), but higher than some values in rivers draining limestone from Tethyan Sedimentary Series (TSS) (0.50-1.30‰) (Tipper et al., 2008). The  $\delta^{44/40}\text{Ca}$  values of the Jinsha River are also consistent with greywacke-draining rivers from the Southern Alps, New Zealand (0.50-1.40‰) (Moore et al., 2013; Pogge von Strandmann et al., 2019b). When compared with other small monolithologic river catchments, the Ca isotopic composition of the Jinsha River is lower than rivers draining granite in La Ronge (1.16-1.33‰) (Holmden and Bélanger, 2010) and parts of the  $\delta^{44/40}\text{Ca}$  values in basaltic rivers from Iceland (0.95-1.37‰) (Hindshaw et al., 2013; Jacobson et al., 2015). Moreover, the  $\delta^{44/40}\text{Ca}$  values of the Jinsha River are higher than that in rivers draining granite in Exmoor (0.50-0.99‰) (Chu et al., 2006) and Strengbach (0.27-0.86‰) (Schmitt et al., 2003).

As a Ca-bearing mineral, gypsum, which is distributed widely in the source

area of the Changjiang River (Fig. 1a), is an important endmember for river dissolved Ca. Five gypsum samples, collected from the source area of the Changjiang River, show variable  $\delta^{44/40}\text{Ca}$  values from 0.24‰ to 0.95‰ with an average of 0.61‰ (Table1). Among them, two gypsum samples collected near the Dangqu River (G1 in Fig. 1a) have lower  $\delta^{44/40}\text{Ca}$  values (0.24-0.27‰). Other three gypsum samples collected near the Tuotuo River (G2 and G3 in Fig. 1a) have higher  $\delta^{44/40}\text{Ca}$  values (0.80-0.95‰).

## 5. Discussion

### 5.1 Sources of dissolved calcium in the Jinsha River

In the Jinsha River basin, potential sources of dissolved Ca are rain water and dissolution of evaporite, silicate and carbonate. And the Ca budget equation of the Jinsha River can be written as follows:

$$(Ca)_{river} = (Ca)_{rain} + (Ca)_{eva} + (Ca)_{sil} + (Ca)_{cab} \quad (3)$$

#### 5.1.1 Atmospheric input

Sample JS-6 has the lowest chloride concentration of 5.8  $\mu\text{mol/L}$  in all river waters, which is consistent with the Cl concentration of local long-term precipitation (0.9-32.7  $\mu\text{mol/L}$ ) (Zhang et al., 2012) and also similar to that of rain water in the Gula area at the middle reach of the Jinsha River (7.9  $\mu\text{mol/L}$ ) (Zhao et al., 2019). Atmospheric input was corrected, assuming that the sample with the lowest chloride concentration (JS-6) obtained its dissolved Cl exclusively from rain water. Elemental ratios in precipitation from (Zhang et al.,

[2012](#)) were used to calculate the concentrations of other major ions (Ca, Mg, Na, K) in rain water. Rain percentages ( $P_{rain}$ ) are calculated by:

$$P_{rain} = \sum cation_{rain} / \sum cation_{river} \quad (4)$$

$$\sum cation_{rain} = Ca_{rain} + Mg_{rain} + Na_{rain} + K_{rain} \quad (5)$$

Results are shown in [Table 3](#). Cations from atmospheric sources account for <5% of total riverine cations. In addition, the long term average Ca/Cl molar ratio in rain waters is 4.34 ([Zhang et al., 2012](#)), and the Ca concentration of rain water is 25.2  $\mu\text{mol/L}$ , then the proportion of Ca derived from rain water to the total of riverine Ca is 2-6%. Previous studies suggested  $\delta^{44/40}\text{Ca}$  values of rain water ranging from -0.34 to 1.30‰ with an average value of  $0.70 \pm 0.16\text{‰}$  ([Han et al., 2019](#); [Schmitt, 2016](#)). The corrected riverine  $\delta^{44/40}\text{Ca}$  are elevated by less than 0.08‰ or lowered by less than 0.02‰, within the long term external precision ( $\pm 0.14\text{‰}$ ). Therefore, atmospheric precipitation has little effect on riverine Ca isotopes.

### 5.1.2 Rock weathering

Based on the lithological distribution in the Jinsha River basin ([Fig. 1a.](#)), silicate 1 (plutonic acid rock), silicate 2 (basaltic volcanic rock), carbonate, and evaporite were chosen as the four main end-members. Meanwhile, strontium isotopes suggest that water chemistry could be controlled by evaporite and silicate as well as carbonate dissolution in agreement with the previous study ([Wu et al., 2011](#)). From upstream to downstream of the Jinsha River, owing to the increasing weathering input from silicates, concentration of dissolved Si in

both mainstream and tributaries increases, which is generally contrary to the decreasing Ca and SO<sub>4</sub> concentration (Fig. 6). However, there is no systemic change of  $\delta^{44/40}\text{Ca}$  along the river. Hence, the Ca isotopic composition of the Jinsha River is not fully controlled by simple mixing between Ca signals of different rock end-members.

The Ca contribution of different rock sources could be calculated by an forward method (Chetelat et al., 2008). Na from silicates of Jinsha tributaries can be obtained by equation as follows:

$$(Na)_{sil} = (Na)_{river}^* - (Cl)_{river}^* \quad (6)$$

Where  $(Na)_{sil}$  represents Na from silicate, and  $(Na)_{river}^*$  and  $(Cl)_{river}^*$  are dissolved Na and Cl in river collected from rain water. However, due to the diverse composition of evaporites (halite, mirabilites, sylvites, borates and sodium carbonate) in the salt lakes near the source area of the Jinsha River (Yu and Tang, 1980), Na from silicates of Jinsha mainstream cannot be obtained based on Eq. (6). A substitute method from (Wu et al., 2008) is conducted to obtain  $(Na)_{sil}$  of mainstream. Assuming that the mainstream and its adjacent tributary have the similar dissolved  $(Na)_{sil}/Si$  ratio, then

$$(Na)_{sil-m} = ((Na)_{sil-t} / (Si)_t) \times (Si)_m \quad (7)$$

Where  $(Na)_{sil-m}$  and  $(Na)_{sil-t}$  are Na from silicate in Jinsha mainstream and tributaries, and  $(Si)_t$  and  $(Si)_m$  represent dissolved Si from Jinsha mainstream and tributaries. Then, dissolved Ca from silicate can be acquired as follows:

$$(Ca)_{sil} = (Na)_{sil} \times (Ca/Na)_{sil} \quad (8)$$

Where  $(Ca)_{sil}$  represents the dissolved Ca from silicate, and  $(Ca/Na)_{sil}$  represents the Ca/Na ratio of silicate widely distributed in the Jinsha river basin. Here  $0.49 \pm 0.3$  was used as the value of  $(Ca/Na)_{sil}$ , which is consistent with the data of the silicate fraction of sediments in the Jinsha River (Wu et al., 2009a). Calculated by Eq. (8), silicate weathering contributes 4-12 % of the riverine Ca; including an uncertainty of 50% (Wu et al., 2009a), this propagates to a 2-24% silicate contribution.

Assuming  $(Ca/SO_4)_{eva}$  (the Ca/SO<sub>4</sub> ratio of evaporites in source area) is 0.95, which is equal to Ca/SO<sub>4</sub> ratios of source rivers (Tuotuo River and Chumaer River) (Wu et al., 2009a), evaporite dissolution contributes 45-81% of dissolved Ca to the Jinsha mainstream and 1-41% to the tributaries. Because mirabilites are abundant in saline lakes near the source of the Jinsha River (Yu and Tang, 1980), pyrite oxidation and sulphuric acid weathering (Chetelat et al., 2008) also can affect the concentration of dissolved SO<sub>4</sub> in the Jinsha River. The calculated  $(Ca)_{eva}$  is the upper limit of evaporite Ca that can be obtained. Through the budget equation (3) of Ca, the contribution of Ca from carbonate weathering ranges from 6 to 43% in the mainstream and 47 to 88% in the tributaries.

In addition, the initial Ca isotopic composition ( $\delta^{44/40}Ca_0$ ) of the Jinsha River water resulting from mixing of different rock sources could be calculated based on a simple mixing equation as follows:

$$\delta^{44/40}Ca_0 = \sum_i \delta^{44/40}Ca_i \times \gamma_i^{Ca} \quad (9)$$

Where  $\delta^{44/40}\text{Ca}_i$  represents the Calcium isotopic composition of source  $i$ , and  $\gamma_i^{\text{Ca}}$  is the mixing proportion of Ca of each source  $i$  (evaporite, silicate 1, silicate 2 and carbonate) contributing to the dissolved load. Fantle and Tipper (2014) compiled over 70 published Ca isotope studies, and obtained that the average values of silicates and carbonates are 0.94‰ and 0.60‰, respectively. Thus, 0.94‰ was chosen as the  $\delta^{44/40}\text{Ca}$  of the silicate endmember in this study. Previous study (Tipper et al., 2006) suggested that the stable Ca isotope composition of limestone in the Tibetan Plateau is 0.61‰, which is close to the average value of worldwide carbonate (0.60‰), and also consistent with the average value of sedimentary rocks of  $0.64 \pm 0.09\text{‰}$  ( $2\sigma_{\text{mean}}$ ;  $N=78$ ) (Ewing et al., 2008; Holmden, 2009; Jacobson and Holmden, 2008; Ludwik Halicz, 1999; Moore et al., 2013; Tipper et al., 2006; Tipper et al., 2008). Therefore, 0.61‰ was chosen as the carbonate endmember in this study. Moreover, we suggest the average value of our gypsum samples (0.61‰) as the  $\delta^{44/40}\text{Ca}$  value of the evaporite endmember, which is not only within the range of gypsum data reported by Hensley (2006) (-0.52‰ to 1.68‰), but also similar to the average  $\delta^{44/40}\text{Ca}$  of anhydrites (0.65‰) suggested by other studies (Amini et al., 2008; Holmden, 2009; Jacobson and Holmden, 2008).

Based on a conventional mixing model (Eq. (9)), the Jinsha River water has a similar theoretical initial  $\delta^{44/40}\text{Ca}$  value of 0.64‰, which is lower than most of the measured values of the Jinsha River. In addition, a negative correlation between  $\delta^{44/40}\text{Ca}$  values and Si/Ca (Fig. 4a) also conflicts with the

conventional mixing model. Hence, Ca isotopes must be fractionated in the Jinsha River.

## 5.2 Potential calcium isotope fractionation processes

### 5.2.1 Vegetable growth

Plants preferentially uptake lighter Ca isotopes, resulting in heavier Ca isotope in the remaining soil solutions. These will therefore elevate riverine Ca isotopes by mixing with river water ([Cenki-Tok et al., 2009](#); [Holmden and Bélanger, 2010](#); [Schmitt et al., 2017](#)).

The topography of the middle and upper sections of the Jinsha River basin is mainly dry and hot valleys with a slow growth rate of plants and low microbial activity in the soil ([Liu, 2016](#)). The Normalized Difference Vegetation Index (NDVI) was used to quantify the density of plant growth in the Jinsha River watershed ([Table 1](#)). Results show that there is no significant relationship between NDVI and the  $\delta^{44/40}\text{Ca}$  values of tributaries, implying that the Ca isotopic signal caused by plant growth may be overprinted by other signals, or its signal is too dilute to elevate the  $\delta^{44/40}\text{Ca}$  values of regional or global scale rivers significantly. Therefore, the effect of plant growth on riverine isotopes may need to be further constrained through tracing the Ca isotopic composition of the Jinsha River in space and time.

### 5.2.2 Mineral dissolution

Mg stable isotope fractionation has been shown to occur not only during

precipitation, but also during the congruent dissolution of magnesite ([Pearce et al., 2012](#)). There is also recent evidence that Ca isotopes can behave in the same way, i.e. exhibiting isotope fractionation during dissolution of calcite, and also at equilibrium (or dynamic equilibrium) ([Oelkers et al., 2019](#)). However, studies on Ca isotope fractionation between silicate minerals and corresponding fluids during water-rock interaction suggested that congruent dissolution of granite minerals at low temperature does not fractionate Ca isotopes ([Cobert et al., 2011](#); [Hindshaw et al., 2011](#); [Ryu et al., 2011](#)). From the above, dissolution of silicate rocks along the Jinsha River are not expected to cause significant Ca isotope fractionation.

### **5.2.3 Clay formation and adsorption**

In the Jinsha River basin, similar clay mineral types exist between tributaries and the main stream ([Zhao et al., 2019](#)), illite and chlorite constitute the main part of the clay minerals in the suspended matter and sediments, followed by montmorillonite and kaolinite ([Ding et al., 2013](#); [Wu et al., 2011](#); [Zhao et al., 2019](#)). And the relative content of illite is 10 times higher than that of montmorillonite ([Wu et al., 2011](#)). This is also consistent with results of previous analyses of clay minerals in surface sediments of the whole Changjiang River basin ([He et al., 2011](#)).

It is hard to constrain the type and amount of the neoformed clay mineral directly. Fortunately, regional climate is linked to clay formation. For instance, illite and chlorite are always formed in dry-cold areas, such as the Changjiang



source area. In contrast, dry and hot environments, like the upper reaches of the Jinsha River, are conducive to the formation of montmorillonite ([He et al., 2011](#)). From upstream to downstream, the climate of the Jinsha river catchment changes from dry-cold to dry-hot climate ([Fig. 7](#)). However, illite and chlorite are also primary components of clay minerals in sediment and suspended matters of rivers under dry-hot condition ([from JS-3 to JS-16 in Fig.7](#)). Combined with the topographical conditions, one of the possible reasons is that pre-weathered material in the dry-cold plateau is being eroded and transported, which is also consistent with the unsaturated state of illite and chlorite in the Jinsha river water ([Table 2](#)). Although the precise location of the formation of clay minerals in rivers is still debated (i.e., soil solutions and/or river particulate material), the saturation indices of clay minerals in river water can reflect the soil water to a degree because of the connectivity between the river and soil solution. Kaolinite and montmorillonite are supersaturated in the Jinsha river water, combined with dry and hot climate condition, part of them are neoformed in the upper reaches of the Jinsha River ([from JS-3 to JS-16 in Fig. 7](#)). However, riverine  $\delta^{44/40}\text{Ca}$  show no systemic change with climate along the riverside. Therefore, the influence of neoformed clay minerals on riverine Ca isotopic composition is minor, assuming that environmental conditions are key in clay mineral formation ([Gislason et al., 1996; Stefánsson and Gislason, 2001](#)).

Previous studies suggested light Ca isotopes are preferentially adsorbed to clays, and the degree of isotopic fractionation depends on types of clay

minerals and their grain sizes ([Brazier et al., 2019](#); [Ockert et al., 2013](#)). Recent Ca isotope adsorption experiments show that no significant isotopic fractionation occurs when Ca isotopes are adsorbed by kaolinite ([Brazier et al., 2019](#)). This is inconsistent with results from Gussone and Dietzel ([2016](#)), who suggested that Ca isotope could be adsorbed strongly onto kaolinite accompanied with  $\Delta^{44/40}\text{Ca}_{\text{ads-fluid}}$  ranging from -1.2~-3.0‰. Due to its fine grain size (<10  $\mu\text{m}$ ), newly formed K-mica may also preferentially adsorb light Ca isotopes, resulting in a positive apparent isotopic fractionation between 0.1‰ and 0.28‰ in the residual solution ([Brazier et al., 2019](#)). Moreover, Ca isotopes adsorbed onto illite cause  $\Delta^{44/40}\text{Ca}_{\text{ads-fluid}}$  ranging from -0.5 to -1.2‰ ([Gussone and Dietzel, 2016](#)), and Ca adsorption and the related isotopic fractionation are thought to be fully reversible ([Brazier et al., 2019](#)). In the Jinsha River waters, k-mica, kaolinite and montmorillonite are supersaturated, and negative correlations were obtained between their saturation index and  $\delta^{44/40}\text{Ca}$  values in tributaries. This conflicts with results from laboratory experiments, which suggest that adsorption by clay minerals leads to heavier  $\delta^{44/40}\text{Ca}$  in residual solutions and there should be a positive correlation between the saturation index of clay minerals and riverine  $\delta^{44/40}\text{Ca}$  values. Therefore, the influence of clay mineral adsorption on Ca isotopic compositions of Jinsha tributaries is minor. In addition, although quantitative evaluation of the impact of Ca adsorption on riverine  $\delta^{44/40}\text{Ca}$  is difficult, Ca flux sorption to the exchangeable fraction may be restrained by excess Na resulting from evaporite dissolution in

the mainstream of the Jinsha River, since it also could impact the  $\delta^{44/40}\text{Ca}$  values if Na is replaced by lighter Ca isotopes preferentially ([Jacobson and Holmden, 2008](#); [Ockert et al., 2013](#)).

#### 5.2.4 Carbonate precipitation

Calcium isotopes are fractionated during authigenic carbonate precipitation from aqueous solutions ([Gussone and Dietzel, 2016](#)), which preferentially takes light Ca isotopes into the solid ([Blättler et al., 2015](#); [Böhm et al., 2012](#); [Gussone et al., 2003](#); [Gussone et al., 2011](#); [Henderson et al., 2006](#); [Holmden, 2009](#); [Jacobson and Holmden, 2008](#); [Nielsen and DePaolo, 2013](#); [Oehlerich et al., 2015](#); [Steuber and Buhl, 2006](#); [Teichert et al., 2005](#); [Tipper et al., 2006](#); [Wang et al., 2012](#); [Wang et al., 2013](#)), consistent with the fractionation displayed by laboratory precipitation experiments of calcite ([Gussone et al., 2003](#); [Gussone et al., 2011](#); [Lemarchand et al., 2004](#); [Tang et al., 2008](#); [Tang et al., 2012](#)). If secondary Ca-bearing minerals are causing the observed fractionation of Ca isotopes in the Jinsha River, the fractionation factor in this process can be calculated ([Hindshaw et al., 2013](#)).

The correlation between metal isotopic compositions ( $\delta^{44/40}\text{Ca}$ ,  $\delta^{26}\text{Mg}$ ) and saturation indices of carbonates could indicate carbonates precipitation ([Fan et al., 2016](#); [Hindshaw et al., 2013](#); [Moore et al., 2013](#); [Pogge von Strandmann et al., 2019a](#); [Pogge von Strandmann et al., 2019b](#); [Pogge von Strandmann et al., 2019c](#); [Tipper et al., 2008](#)). The positive relationship between riverine  $\delta^{44/40}\text{Ca}$  values with CSI and Sr/Ca ratios ([Fig. 8a and b](#)), implies that

carbonates precipitation may elevate the Ca isotopic compositions of the Jinsha River waters.  $f_{Ca}$  represents the fraction of Ca still in solution. If  $f_{Ca}$  equals to 1, there will be no Ca incorporated into secondary minerals after its initial dissolution. In contrast, all Ca from primary mineral dissolution will precipitate as secondary minerals when  $f_{Ca}$  has a value of 0. Assuming that the release of Ca and Na from bed rocks is congruent,  $f_{Ca}$  can be calculated as below:

$$f_{Ca} = \left( \frac{Ca}{Na} \right)_{river} / \left( \frac{Ca}{Na} \right)_0 \quad (10)$$

Previous research suggested that Ca/Na (molar) values of sediment of the Jinsha mainstream change slightly from Benzilan (3.46) to Panzhihua (2.85) with an average value of 3.20 (Wu et al., 2011). Assuming the  $(Ca/Na)_0$  of Jinsha mainstream equals 3.20, then  $f_{Ca}$  has a range from 0.16 to 0.34. Similarly,  $(Ca/Na)_0$  of Tongtianhe (JS-1) equals 5.6 and its  $f_{Ca}$  equals 0.07. Additionally,  $f_{Ca}$  values of the Jinsha mainstream show significant correlation with CSI ( $R^2 = 0.82$ ) and pH values ( $R^2 = 0.93$ ), implying the amount of carbonate precipitation in the Jinsha mainstream ranges from 66% to 93% with an average of 75%.

Fig. 9a shows a relationship between measured riverine  $\delta^{44/40}Ca$  values and Ca/Na ratios of river samples. Both Rayleigh distillation model and equilibrium fractionation processes are examined in the Jinsha mainstream samples, and corresponding fractionation factor values are calculated. According to the equilibrium fractionation model, the Ca isotope composition can be modelled as:

$$\delta^{44/40}Ca_{river} = \delta^{44/40}Ca_0 - 1000(\alpha - 1) \times (1 - f_{Ca}) \quad (11)$$

In addition, to evaluate fractionation factors of the Rayleigh distillation model, a standard approach is conducted as follows ([Dellinger et al., 2015](#); [Hindshaw et al., 2013](#); [Pogge von Strandmann et al., 2017](#); [Pogge von Strandmann et al., 2012](#); [Zhao et al., 2019](#)):

$$\delta^{44/40}Ca_{river} = \delta^{44/40}Ca_0 + 1000(\alpha - 1) \times \ln(f_{Ca}) \quad (12)$$

where  $\delta^{44/40}Ca_{river}$  corresponds to the Ca isotope composition of river water, and mainstream and tributaries of the Jinsha River have similar initial isotopic compositions ( $\delta^{44/40}Ca_0 = 0.64\text{‰}$ ).

Different fractionation models lead to variable fractionation factors ( $\alpha$ ). For the Jinsha mainstream, the range of Ca isotope Rayleigh fractionation factor is 0.99961-0.99983, with a median of 0.99976, which is consistent with basaltic river data that follow a Rayleigh relationship in Iceland (0.9998) ([Hindshaw et al., 2013](#)). Whereas, equilibrium fractionation results in a range of 0.99935-0.99963, with a best fit fractionation factor value of 0.99953, which is a little bit higher than the fractionation factor into inorganic calcite ( $\alpha = 0.9990$ -0.9995) ([Gussone et al., 2005](#)); the difference may come from diverse precipitation rate, difference temperature and solution chemistry.

Selecting 0.99953 as the  $\alpha$  value of the equilibrium fractionation,  $f_{Ca}$  values of the Jinsha tributaries range from 0.47 to 0.90 based on Eq. (11), which corresponds to the amount of Ca precipitation, which ranges from 10% to 53%, with an average value of 35%. Similarly, choosing 0.99973 as the  $\alpha$  value of the

Rayleigh fractionation model, according to equation (12), the range of  $f_{Ca}$  of the Jinsha tributaries is 0.12-0.66, and the corresponding precipitation range is 34%-88%, with an average of 72%. Moreover, using the batch fractionation model and the optimal fractionation factor, the  $f_{Ca}$  of the main stream of the Jinsha River is 0.49-0.66, which is closer to the  $f_{Ca}$  calculated based on the sediment composition of the riverbed. However, using the Rayleigh fractionation model and its best fit  $\alpha$  value could obtain the  $f_{Ca}$  of the Jinsha River mainstream with a range of 0.02-0.13, which overestimates the Ca precipitation amount in the main stream of the Jinsha River. In addition, Rayleigh fractionation requires a closed system, while the river is an open system, so the equilibrium fractionation model is more appropriate. Therefore, the amount of carbonate precipitation in the tributary has a dissolved Ca uptake range of 10%-53%. Considering the range of fractionation factor is from 0.99935 to 0.99963, the uncertainty of the evaluation of the amount of carbonate precipitation is ~10%.

From the above, we suggest that carbonate precipitation has taken place in the Jinsha River, which is congruous with the results obtained by Zhao et al. (2019) through the study of Mg isotopes in the same river.

### 5.3 Effect of evaporite weathering on Ca isotopes

In Section 5.2.2,  $f_{Ca}$  values of the Jinsha River mainstream are lower than those of the tributaries, which may indicate more carbonate has precipitated in

the mainstream. One of the reasons is that weathering of Ca-bearing evaporites, mainly gypsum, which are widely distributed in the source area of the Jinsha River, releases more  $\text{Ca}^{2+}$  into the river water, resulting in a higher saturation index of carbonate (above zero), which gives rise to precipitation of carbonate and elevated Ca isotopic compositions of the mainstream river water, since secondary carbonates incorporate lighter Ca isotopes preferentially ([Gussone et al., 2003](#); [Gussone et al., 2011](#); [Lemarchand et al., 2004](#); [Tang et al., 2008](#); [Tang et al., 2012](#); [Tipper et al., 2006](#)).

In this study, we evaluated the amount of calcium carbonate precipitation, and then assessed the effect of evaporite dissolution on calcium carbonate precipitation and river Ca isotopes. The  $f_{\text{Ca}}$  values of the tributaries are variable, ranging from 0.47 to 0.90 with an uncertainty of  $\sim 0.1$ , which indicates that the proportion of precipitated Ca ranges from 0% to 63% with the average of 35%. However,  $f_{\text{Ca}}$  in the mainstream ranges from 0.07 to 0.34 with an average of 0.25, which suggests at least 66% of dissolved Ca has precipitated. This result is lower than that of the tributaries, but in good agreement with previous studies which indicated up to 70% of Ca in Himalayan rivers was removed through carbonate precipitation ([Bickle et al., 2005](#); [Jacobson et al., 2002](#)).

Widespread limestone in the Jinsha River Basin releases plenty of dissolved Ca into the river, and, combined with an arid climate, provides the necessary conditions for the precipitation of carbonate. Weathering of evaporite releases more dissolved Ca into river water and increases the precipitation of

carbonate by ~30%. Note that plants growth and clay mineral adsorption and/or incorporation also uptake more Ca than Na, which will reduce riverine Ca/Na ratios and  $f_{Ca}$  values. Therefore, what we have obtained is the upper limit of the amount of precipitation.

Further, the influence of evaporite weathering still needs to be evaluated. Ca isotope ratios at the source of the Changjiang river, published by Tipper et al. ([2010](#)), are 1.04‰ in summer and by Zhu and MacDougall ([1988](#)) as 1.25‰, which is consistent with our results (1.11‰, JS-1). However, Ca isotope ratios at the river mouth have an average of 0.77‰, which is similar to the average value (0.80‰) of the tributaries of the Jinsha River. This suggests that evaporite weathering in the upper reaches of the Changjiang river do not affect its Ca isotopic composition entering into the ocean. Therefore, evaporite weathering could fractionate Ca isotope significantly, but this signal appears to be overprinted by other processes further downstream. In most cases, the influence of evaporite dissolution is limited and only could affect the  $\delta^{44/40}Ca$  of small and regional rivers. However, some large rivers may also be affected by evaporite weathering and have higher  $\delta^{44/40}Ca$  values than others, such as the Yellow River, which has high Ca isotope ratios in both summer and winter at its estuary ([Tipper et al., 2010](#)). Additionally, while investigating the evolution of paleoclimate using stable Ca isotopes, it may necessary to consider the effect of evaporites weathering. For example, when the paleo-temperature is high, the enhanced evaporation leads to the extensive distribution of evaporites, which



elevates  $\delta^{44/40}\text{Ca}$  value of the continental weathering flux, and then affect the global Ca mass balance.

## Conclusion

This study investigated chemical weathering and solute sources constrained by calcium and strontium isotopes in the upper reaches of the Changjiang River. Hydrochemistry of the mainstream is different from that of tributaries, and the contribution order of solute sources is evaporites > carbonates > silicates for the mainstream, while carbonates > silicates > evaporites for tributaries.

The  $\delta^{44/40}\text{Ca}$  of the dissolved load in the upper reaches of the Jinsha River ranges from 0.68‰ to 1.11‰ with an average of 0.87‰. The effects of atmospheric input and biological input on the Ca isotope ratio of rivers are minor. The conventional mixing of different rock sources cannot fully explain the Ca isotope ratio of the Jinsha River and secondary processes must be invoked. Owing to a weak negative correlation between the Ca isotope ratios and the saturation indices of silicate clay minerals, adsorption or incorporation is not the main factor that raises the Ca isotope ratio of the river. Combined with the positive correlation between calcite saturation indices and  $\delta^{44/40}\text{Ca}$  values, we believe that calcium carbonate precipitation is the cause of elevated Ca isotope ratios. Moreover, the Equilibrium fractionation model can be used to explaining Ca isotopic compositions of the Jinsha River, and the calculated fractionation

factors are between 0.99935 and 0.99965, which are similar to fractionation known to be caused by calcite precipitation.

Evaporite (mainly gypsum) weathering controls the amount of carbonate precipitation indirectly through the release of  $\text{Ca}^{2+}$  into the river water which elevates the CSI value. In the dry and cold plateau climate, at least 66% Ca was removed from the mainstream of the Jinsha River while the average value is ~35% in the tributaries, resulting in a heavier Ca isotope ratio in the main stream than in the tributaries. However, the impact of evaporite weathering on carbon budgets of rivers still needs more related research to test.

## **Acknowledgments**

This work was funded by the 2nd Tibetan Plateau Scientific Expedition and Research (2019QZKK0707), the Tianjin Science Fund for Distinguished Young Scholars (18JCJQJC46200), the National Key R&D Program of China (2016YFA0601002), National Natural Science Foundation of China (41571130072), UK-China Joint Research and Innovation Partnership Fund PhD Placement Programme (CSC NO. 201806250237) and Tianjin University's Top Doctoral Thesis International Cultivation Programme. PPvS is funded by ERC Consolidator grant 682760 CONTROLPASTCO<sub>2</sub>. We thank Prof. Wang Zheng , Dr. Liang Zhang , Dr. Liang Qiu and Dr. Fujun Yue for their insightful discussions during the manuscript preparation. We also thank Prof. Yucai Song for providing gypsum samples. We appreciate the insightful comments and

constructive suggestions from the editor and the anonymous reviewers.

## Reference

- Amini, M. et al., 2008. Calcium isotope ( $\delta^{44}/^{40}\text{Ca}$ ) fractionation along hydrothermal pathways, Logatchev field (Mid-Atlantic Ridge, 14°45'N). *Geochimica et Cosmochimica Acta*, 72(16): 4107-4122, doi:10.1016/j.gca.2008.05.055.
- Belshaw, N., Zhu, X., Guo, Y., O'Nions, R., 2000. High precision measurement of iron isotopes by plasma source mass spectrometry. *International Journal of Mass Spectrometry*, 197(1-3): 191-195, doi:10.1016/S1387-3806(99)00245-6.
- Berner, E.K., Berner, R.A., 2012. Global environment: water, air, and geochemical cycles.
- Berner, R.A., 2003. The long-term carbon cycle, fossil fuels and atmospheric composition. *Nature*, 426: 323-326, doi:10.1038/nature02131.
- Berner, R.A., Lasaga, A.C., Garrels, R.M., 1983. The carbonate-silicate geochemical cycle and its effect on atmospheric carbon-dioxide over the past 100 million years. *American Journal of Science*, 283: 641-683, doi:10.2475/ajs.283.7.641.
- Bickle, M.J. et al., 2005. Relative contributions of silicate and carbonate rocks to riverine Sr fluxes in the headwaters of the Ganges. *Geochimica et Cosmochimica Acta*, 69(9): 2221-2240, doi:10.1016/j.gca.2004.11.019.
- Blättler, C.L., Higgins, J.A., 2014. Calcium isotopes in evaporites record variations in Phanerozoic seawater  $\text{SO}_4$  and Ca. *Geology*, 42(8): 711-714, doi:10.1130/g35721.1.
- Blättler, C.L., Miller, N.R., Higgins, J.A., 2015. Mg and Ca isotope signatures of authigenic dolomite in siliceous deep-sea sediments. *Earth and Planetary Science Letters*, 419: 32-42, doi:10.1016/j.epsl.2015.03.006.
- Böhm, F. et al., 2012. Strontium isotope fractionation of planktic foraminifera and inorganic calcite. *Geochimica et Cosmochimica Acta*, 93: 300-314, doi:10.1016/j.gca.2012.04.038.
- Brazier, J.-M. et al., 2019. Calcium isotopic fractionation during adsorption onto and desorption from soil phyllosilicates (kaolinite, montmorillonite and muscovite). *Geochimica et Cosmochimica Acta*, 250: 324-347, doi:10.1016/j.gca.2019.02.017.
- Cenki-Tok, B. et al., 2009. The impact of water-rock interaction and vegetation on calcium isotope fractionation in soil- and stream waters of a small, forested catchment (the Strengbach case). *Geochimica et Cosmochimica Acta*, 73(8): 2215-2228, doi:10.1016/j.gca.2009.01.023.
- Chetelat, B. et al., 2008. Geochemistry of the dissolved load of the Changjiang Basin rivers: Anthropogenic impacts and chemical weathering. *Geochimica et Cosmochimica Acta*, 72(17): 4254-4277, doi:10.1016/j.gca.2008.06.013.
- Chu, N.-C., Henderson, G.M., Belshaw, N.S., Hedges, R.E.M., 2006. Establishing the potential of Ca isotopes as proxy for consumption of dairy products. *Applied Geochemistry*, 21(10): 1656-1667, doi:10.1016/j.apgeochem.2006.07.003.
- Cobert, F. et al., 2011. Experimental identification of Ca isotopic fractionations in higher plants. *Geochimica et Cosmochimica Acta*, 75(19): 5467-5482, doi:10.1016/j.gca.2011.06.032.
- Dellinger, M. et al., 2015. Riverine Li isotope fractionation in the Amazon River basin controlled by

the weathering regimes. *Geochimica et Cosmochimica Acta*, 164: 71-93, doi:10.1016/j.gca.2015.04.042.

DePaolo, D.J., 2004. Calcium Isotopic Variations Produced by Biological, Kinetic, Radiogenic and Nucleosynthetic Processes. *Reviews in Mineralogy and Geochemistry*, 55: 255-288, doi:10.2138/gsrmg.55.1.255.

Ding, T. et al., 2013. The contents and mineral and chemical compositions of suspended particulate materials in the Yangtze River, and their geological and environmental implacations. *Acta Geologica Sinica*, 87(5): 634-660 (*In Chinese with English abstract*).

Ewing, S.A. et al., 2008. Non-biological fractionation of stable Ca isotopes in soils of the Atacama Desert, Chile. *Geochimica et Cosmochimica Acta*, 72(4): 1096-1110, doi:10.1016/j.gca.2007.10.029.

Fan, B. et al., 2016. The geochemical behavior of Mg isotopes in the Huanghe basin, China. *Chemical Geology*, 426: 19-27, doi:10.1016/j.chemgeo.2016.01.005.

Fantle, M.S., 2010. Evaluating the Ca isotope proxy. *American Journal of Science*, 310(3): 194-230, doi:10.2475/03.2010.03.

Fantle, M.S., 2015. Calcium isotopic evidence for rapid recrystallization of bulk marine carbonates and implications for geochemical proxies. *Geochimica et Cosmochimica Acta*, 148: 378-401, doi:10.1016/j.gca.2014.10.005.

Fantle, M.S., DePaolo, D.J., 2005. Variations in the marine Ca cycle over the past 20 million years. *Earth and Planetary Science Letters*, 237(1-2): 102-117, doi:10.1016/j.epsl.2005.06.024.

Fantle, M.S., Tipper, E.T., 2014. Calcium isotopes in the global biogeochemical Ca cycle: Implications for development of a Ca isotope proxy. *Earth-Science Reviews*, 129: 148-177, doi:10.1016/j.earscirev.2013.10.004.

Farkaš, J. et al., 2007. Calcium isotope record of Phanerozoic oceans: Implications for chemical evolution of seawater and its causative mechanisms. *Geochimica et Cosmochimica Acta*, 71(21): 5117-5134, doi:10.1016/j.gca.2007.09.004.

Farkaš, J., Déjeant, A., Novák, M., Jacobsen, S.B., 2011. Calcium isotope constraints on the uptake and sources of  $\text{Ca}^{2+}$  in a base-poor forest: A new concept of combining stable ( $\delta^{44/42}\text{Ca}$ ) and radiogenic ( $\epsilon\text{Ca}$ ) signals. *Geochimica et Cosmochimica Acta*, 75(22): 7031-7046, doi:10.1016/j.gca.2011.09.021.

Gaillardet, J., Allegre, C.J., Dupre, B., Louvat, P., 1999. Global silicate weathering and  $\text{CO}_2$  consumption rates deduced from the chemistry of large rivers. *Chemical Geology*, 159: 3-30, doi:10.1016/S0009-2541(99)00031-5.

Gaillardet, J., Calmels, D., Romero-Mujalli, G., Zakharova, E., Hartmann, J., 2018. Global climate control on carbonate weathering intensity. *Chemical Geology*, doi:10.1016/j.chemgeo.2018.05.009.

Galy, A., France-Lanord, C., 1999. Weathering processes in the Ganges–Brahmaputra basin and the riverine alkalinity budget. *Chemical Geology*, 159: 31-60, doi:10.1016/S0009-2541(99)00033-9.

Gislason, S.R., Arnorsson, S., Armannsson, H., 1996. Chemical weathering of basalt in Southwest Iceland; effects of runoff, age of rocks and vegetative/glacial cover. *American Journal of Science*, 296(8): 837-907, doi:10.2475/ajs.296.8.837.

Gussone, N. et al., 2005. Calcium isotope fractionation in calcite and aragonite. *Geochimica et Cosmochimica Acta*, 69(18): 4485-4494, doi:10.1016/j.gca.2005.06.003.

813 Gussone, N., Dietzel, M., 2016. Calcium Isotope Fractionation During Mineral Precipitation from  
814 Aqueous Solution, in : Nikolaus Gussone et al., Calcium Stable Isotope Geochemistry.  
815 Advances in Isotope Geochemistry. Springer, Berlin, Heidelberg.

816 Gussone, N. et al., 2003. Model for kinetic effects on calcium isotope fractionation ( $\delta^{44}\text{Ca}$ ) in  
817 inorganic aragonite and cultured planktonic foraminifera. *Geochimica et Cosmochimica*  
818 *Acta*, 67(7): 1375-1382, doi:10.1016/s0016-7037(02)01296-6.

819 Gussone, N., Nehrke, G., Teichert, B.M.A., 2011. Calcium isotope fractionation in ikaite and vaterite.  
820 *Chemical Geology*, 285(1-4): 194-202, doi:10.1016/j.chemgeo.2011.04.002.

821 Han, G., Song, Z., Tang, Y., Wu, Q., Wang, Z., 2019. Ca and Sr isotope compositions of rainwater  
822 from Guiyang city, Southwest China: Implication for the sources of atmospheric aerosols  
823 and their seasonal variations. *Atmospheric Environment*, 214,  
824 doi:10.1016/j.atmosenv.2019.116854.

825 Harouaka, K., Eisenhauer, A., Fantle, M.S., 2014. Experimental investigation of Ca isotopic  
826 fractionation during abiotic gypsum precipitation. *Geochimica et Cosmochimica Acta*, 129:  
827 157-176, doi:10.1016/j.gca.2013.12.004.

828 He, M.-Y., Zheng, H.-B., Huang, X.-T., Jia, J.-T., Li, L., 2011. Clay Mineral Assemblages in the  
829 Yangtze Drainage and Provenance Implications. *Acta Sedimentologica Sinica*, 29(3): 544 -  
830 551 (*in Chinese with English abstract*). doi:10.14027/j.cnki.cjxb.2011.03.006.

831 Henderson, G.M., Chu, N.C., Bayon, G., Benoit, M., 2006.  $\delta^{44/42}\text{Ca}$  in gas hydrates, porewaters and  
832 authigenic carbonates from Niger Delta sediments. *Geochimica et Cosmochimica Acta*,  
833 70(18), doi:10.1016/j.gca.2006.06.493.

834 Hensley, T., 2006. Calcium isotope variation in marine evaporates and carbonates, applications to  
835 late Miocene Mediterranean brine chemistry and late Cenozoic calcium cycling in the  
836 oceans, UC San Diego.

837 Heuser, A., Schmitt, A.-D., Gussone, N., Wombacher, F., 2016. Analytical Methods. In: Nikolaus  
838 Gussone et al., Calcium Stable Isotope Geochemistry. Advances in Isotope Geochemistry.  
839 Springer, Berlin, Heidelberg.

840 Hindshaw, R.S., Bourdon, B., Pogge von Strandmann, P.A.E., Vigier, N., Burton, K.W., 2013. The  
841 stable calcium isotopic composition of rivers draining basaltic catchments in Iceland. *Earth*  
842 *and Planetary Science Letters*, 374: 173-184, doi:10.1016/j.epsl.2013.05.038.

843 Hindshaw, R.S. et al., 2012. Calcium isotope fractionation in alpine plants. *Biogeochemistry*, 112(1-  
844 3): 373-388, doi:10.1007/s10533-012-9732-1.

845 Hindshaw, R.S., Reynolds, B.C., Wiederhold, J.G., Kretzschmar, R., Bourdon, B., 2011. Calcium  
846 isotopes in a proglacial weathering environment: Damma glacier, Switzerland. *Geochimica*  
847 *et Cosmochimica Acta*, 75(1): 106-118, doi:10.1016/j.gca.2010.09.038.

848 Holmden, C., 2009. Ca isotope study of Ordovician dolomite, limestone, and anhydrite in the  
849 Williston Basin: Implications for subsurface dolomitization and local Ca cycling. *Chemical*  
850 *Geology*, 268(3-4): 180-188, doi:10.1016/j.chemgeo.2009.08.009.

851 Holmden, C., Bélanger, N., 2010. Ca isotope cycling in a forested ecosystem. *Geochimica et*  
852 *Cosmochimica Acta*, 74(3): 995-1015, doi:10.1016/j.gca.2009.10.020.

853 Jacobson, A.D., Blum, J.D., Chamberlain, C.P., Poage, M.A., Sloan, V.F., 2002. Ca/Sr and Sr isotope  
854 systematics of a Himalayan glacial chronosequence: Carbonate versus silicate weathering  
855 rates as a function of landscape surface age. *Geochimica et Cosmochimica Acta*, 66(1):  
856 13-27, doi:10.1016/S0016-7037(01)00755-4.

857 Jacobson, A.D., Grace Andrews, M., Lehn, G.O., Holmden, C., 2015. Silicate versus carbonate  
858 weathering in Iceland: New insights from Ca isotopes. *Earth and Planetary Science Letters*,  
859 416: 132-142, doi:10.1016/j.epsl.2015.01.030.

860 Jacobson, A.D., Holmden, C., 2008.  $\delta^{44}\text{Ca}$  evolution in a carbonate aquifer and its bearing on the  
861 equilibrium isotope fractionation factor for calcite. *Earth and Planetary Science Letters*,  
862 270(3-4): 349-353, doi:10.1016/j.epsl.2008.03.039.

863 Jacobson, A.D., Wasserburg, G.J., 2005. Anhydrite and the Sr isotope evolution of groundwater in  
864 a carbonate aquifer. *Chemical Geology*, 214(3-4): 331-350,  
865 doi:10.1016/j.chemgeo.2004.10.006.

866 Lehn, G.O. et al., 2017. Constraining seasonal active layer dynamics and chemical weathering  
867 reactions occurring in North Slope Alaskan watersheds with major ion and isotope ( $\delta^{34}\text{S}_{\text{SO}_4}$ ,  
868  $\delta^{13}\text{C}_{\text{DIC}}$ ,  $^{87}\text{Sr}/^{86}\text{Sr}$ ,  $\delta^{44/40}\text{Ca}$ , and  $\delta^{44/42}\text{Ca}$ ) measurements. *Geochimica et Cosmochimica Acta*,  
869 217: 399-420, doi:10.1016/j.gca.2017.07.042.

870 Lemarchand, D., Wasserburg, G.J., Papanastassiou, D.A., 2004. Rate-controlled calcium isotope  
871 fractionation in synthetic calcite. *Geochimica et Cosmochimica Acta*, 68(22): 4665-4678,  
872 doi:10.1016/j.gca.2004.05.029.

873 Liu, X.-W., 2016. Preliminary study on characteristics of Meteorological factors and runoff Law in  
874 Jinsha River Basin (*in Chinese with English abstract*).

875 Lu, L., Wang, Q., Wang, G.-Q., Liu, Y.-L., Liu, C.-S., 2016. Trend of Climate Change over the Recent  
876 60 Years and its Hydrological Responses for Jinsha River Basin. *Journal of Noah China*  
877 *University of Water Resources and Electric Power (Natural Science Edition)*, 37(5): 16-21  
878 (*in Chinese with English abstract*).

879 Ludwik Halicz, A.G., Nick S. Belshaw and R. Keith O'Nions, 1999. High-precision measurement of  
880 calcium isotopes in carbonates and related materials by multiple collector inductively  
881 coupled plasma mass spectrometry (MC-ICP-MS). *Journal of Analytical Atomic*  
882 *Spectrometry*, 14: 1835-1838.

883 Marie-Laure Bagard et al., 2013. Biogeochemistry of stable Ca and radiogenic Sr isotopes in a  
884 larch-covered permafrost-dominated watershed of Central Siberia. *Geochimica et*  
885 *Cosmochimica Acta*, 114: 169-187, doi:10.1016/j.gca.2013.03.038.

886 Marie-Laure Bagard et al., 2011. Seasonal variability of element fluxes in two Central Siberian rivers  
887 draining high latitude permafrost dominated areas. *Geochimica et Cosmochimica Acta*,  
888 75(12): 3335-3357, doi:10.1016/j.gca.2011.03.024.

889 Moore, J., Jacobson, A.D., Holmden, C., Craw, D., 2013. Tracking the relationship between  
890 mountain uplift, silicate weathering, and long-term  $\text{CO}_2$  consumption with Ca isotopes:  
891 Southern Alps, New Zealand. *Chemical Geology*, 341: 110-127,  
892 doi:10.1016/j.chemgeo.2013.01.005.

893 Nan, X. et al., 2015. High-precision barium isotope measurements by MC-ICP-MS. *Journal of*  
894 *Analytical Atomic Spectrometry*, 30(11): 2307-2315, doi:10.1039/c5ja00166h.

895 Nielsen, L.C., DePaolo, D.J., 2013. Ca isotope fractionation in a high-alkalinity lake system: Mono  
896 Lake, California. *Geochimica et Cosmochimica Acta*, 118: 276-294,  
897 doi:10.1016/j.gca.2013.05.007.

898 Noh, H., Huh, Y., Qin, J., Ellis, A., 2009. Chemical weathering in the Three Rivers region of Eastern  
899 Tibet. *Geochimica et Cosmochimica Acta*, 73(7): 1857-1877,  
900 doi:10.1016/j.gca.2009.01.005.

Ockert, C., Gussone, N., Kaufhold, S., Teichert, B.M.A., 2013. Isotope fractionation during Ca exchange on clay minerals in a marine environment. *Geochimica et Cosmochimica Acta*, 112: 374-388, doi:10.1016/j.gca.2012.09.041.

Oehlerich, M. et al., 2015. Lateglacial and Holocene climatic changes in south-eastern Patagonia inferred from carbonate isotope records of Laguna Potrok Aike (Argentina). *Quaternary Science Reviews*, 114: 189-202, doi:10.1016/j.quascirev.2015.02.006.

Oelkers, E.H., Pogge von Strandmann, P.A.E., Mavromatis, V., 2019. The rapid resetting of the Ca isotopic signatures of calcite at ambient temperature during its congruent dissolution, precipitation, and at equilibrium. *Chemical Geology*, 512: 1-10, doi:10.1016/j.chemgeo.2019.02.035.

Owen, R.A. et al., 2016. Calcium isotopes in caves as a proxy for aridity: Modern calibration and application to the 8.2 kyr event. *Earth and Planetary Science Letters*, 443: 129-138, doi:10.1016/j.epsl.2016.03.027.

Parkhurst, D.L., Appelo, C.A.J., 1999. User's guide to PHREEQC (Version 2): A computer program for speciation, batch-reaction, one-dimensional transport, and inverse geochemical calculations. Water-Resources Investigations Report.

Pearce, C.R., Saldi, G.D., Schott, J., Oelkers, E.H., 2012. Isotopic fractionation during congruent dissolution, precipitation and at equilibrium: Evidence from Mg isotopes. *Geochimica et Cosmochimica Acta*, 92: 170-183, doi:10.1016/j.gca.2012.05.045.

Pogge von Strandmann, P.A.E. et al., 2019a. Rapid CO<sub>2</sub> mineralisation into calcite at the CarbFix storage site quantified using calcium isotopes. *Nature Communication*, 10(1): 1983, doi:10.1038/s41467-019-10003-8.

Pogge von Strandmann, P.A.E., Frings, P.J., Murphy, M.J., 2017. Lithium isotope behaviour during weathering in the Ganges Alluvial Plain. *Geochimica et Cosmochimica Acta*, 198: 17-31, doi:10.1016/j.gca.2016.11.017.

Pogge von Strandmann, P.A.E., Hendry, K.R., Hatton, J.E., Robinson, L.F., 2019b. The Response of Magnesium, Silicon, and Calcium Isotopes to Rapidly Uplifting and Weathering Terrains: South Island, New Zealand. *Frontiers in Earth Science*, 7, doi:10.3389/feart.2019.00240.

Pogge von Strandmann, P.A.E., Jenkyns, H.C., Woodfine, R.G., 2013. Lithium isotope evidence for enhanced weathering during Oceanic Anoxic Event 2. *Nature Geoscience*, 6(8): 668-672, doi:10.1038/ngeo1875.

Pogge von Strandmann, P.A.E., Olsson, J., Luu, T.-H., Gislason, S.R., Burton, K.W., 2019c. Using Mg Isotopes to Estimate Natural Calcite Compositions and Precipitation Rates During the 2010 Eyjafjallajökull Eruption. *Frontiers in Earth Science*, 7, doi:10.3389/feart.2019.00006.

Pogge von Strandmann, P.A.E. et al., 2012. Lithium, magnesium and silicon isotope behaviour accompanying weathering in a basaltic soil and pore water profile in Iceland. *Earth and Planetary Science Letters*, 339-340: 11-23, doi:10.1016/j.epsl.2012.05.035.

Rocha, C.L.D.L., DePaolo, D.J., 2000. Isotopic evidence for variations in the marine calcium cycle over the Cenozoic. *Science*, 289(5482): 1176-1178, doi:10.1126/science.289.5482.1176.

Rudnick, R.L., Gao, S., 2014. Composition of the Continental Crust, in : Karl Turekian and Heinrich Holland, *Treatise on Geochemistry*, pp. 1-51.

Russell, W.A., Papanastassiou, D.A., Tombrello, T.A., 1978. Ca isotope fractionation on the Earth and other solar system materials. 42: 1075-1090, doi:0016-7037/78/0801-1075\$02.00/0.

Ryu, J.-S., Jacobson, A.D., Holmden, C., Lundstrom, C., Zhang, Z., 2011. The major ion,  $\delta^{44/40}\text{Ca}$ ,

945  $\delta^{44/42}\text{Ca}$ , and  $\delta^{26/24}\text{Mg}$  geochemistry of granite weathering at pH=1 and T=25°C: power-  
 946 law processes and the relative reactivity of minerals. *Geochimica et Cosmochimica Acta*,  
 947 75(20): 6004-6026, doi:10.1016/j.gca.2011.07.025.  
 948 Schmitt, A.-D., 2016. Earth-Surface Ca Isotopic Fractionations, in : Nikolaus Gussone et al, Calcium  
 949 Stable Isotope Geochemistry. *Advances in Isotope Geochemistry*. Springer, Berlin,  
 950 Heidelberg, pp. 145-172.  
 951 Schmitt, A.-D., Chabaux, F., Stille, P., 2003. The calcium riverine and hydrothermal isotopic fluxes  
 952 and the oceanic calcium mass balance. *Earth and Planetary Science Letters*, 213(3-4): 503-  
 953 518, doi:10.1016/s0012-821x(03)00341-8.  
 954 Schmitt, A.-D., Gangloff, S., Labolle, F., Chabaux, F., Stille, P., 2017. Calcium biogeochemical cycle  
 955 at the beech tree-soil solution interface from the Strengbach CZO (NE France): insights  
 956 from stable Ca and radiogenic Sr isotopes. *Geochimica et Cosmochimica Acta*, 213: 91 -  
 957 109, doi:10.1016/j.gca.2017.06.039.  
 958 Stefánsson, A., Gíslason, S.R., 2001. Chemical Weathering of Basalts, Southwest Iceland: Effect of  
 959 Rock Crystallinity and Secondary Minerals on Chemical Fluxes to the Ocean. *American*  
 960 *Journal of Science*, 301(6): 513-556, doi:10.2475/ajs.301.6.513.  
 961 Steuber, T., Buhl, D., 2006. Calcium-isotope fractionation in selected modern and ancient marine  
 962 carbonates. *Geochimica et Cosmochimica Acta*, 70(22): 5507-5521,  
 963 doi:10.1016/j.gca.2006.08.028.  
 964 Su, Z.-H., Chen, W.-Z., 2016. Runoff in Source Region of the Yangtze River in Recent 60 Years:  
 965 Variation Characteristics and Trend Analysis. *Chinese Agricultural Science Bulletin*, 32(34):  
 966 166-171 (*in Chinese with English abstract*).  
 967 Sun, J. et al., 2019. A one-column separation of Ca and Sr for isotopic analysis using MC-ICPMS  
 968 Goldschmidt.  
 969 Tang, J., Dietzel, M., Böhm, F., Köhler, S.J., Eisenhauer, A., 2008.  $\text{Sr}^{2+}/\text{Ca}^{2+}$  and  $^{44}\text{Ca}/^{40}\text{Ca}$  fractionation  
 970 during inorganic calcite formation: II. Ca isotopes. *Geochimica et Cosmochimica Acta*,  
 971 72(15): 3733-3745, doi:10.1016/j.gca.2008.05.033.  
 972 Tang, J. et al., 2012.  $\text{Sr}^{2+}/\text{Ca}^{2+}$  and  $^{44}\text{Ca}/^{40}\text{Ca}$  fractionation during inorganic calcite formation: III.  
 973 Impact of salinity/ionic strength. *Geochim Cosmochim Acta*, 77(C): 432-443,  
 974 doi:10.1016/j.gca.2011.10.039.  
 975 Teichert, B.M.A., Gussone, N., Eisenhauer, A., Bohrmann, G., 2005. Clathrites: Archives of near-  
 976 seafloor pore-fluid evolution ( $\delta^{44/40}\text{Ca}$ ,  $\delta^{13}\text{C}$ ,  $\delta^{18}\text{O}$ ) in gas hydrate environments. *Geology*,  
 977 33(3): 213-216, doi:10.1130/g21317.1.  
 978 Tipper, E., Galy, A., Bickle, M., 2006. Riverine evidence for a fractionated reservoir of Ca and Mg on  
 979 the continents: Implications for the oceanic Ca cycle. *Earth and Planetary Science Letters*,  
 980 247(3-4): 267-279, doi:10.1016/j.epsl.2006.04.033.  
 981 Tipper, E.T. et al., 2010. Calcium isotope ratios in the world's largest rivers: A constraint on the  
 982 maximum imbalance of oceanic calcium fluxes. *Global Biogeochemical Cycles*, 24(3),  
 983 doi:10.1029/2009gb003574.  
 984 Tipper, E.T., Galy, A., Bickle, M.J., 2008. Calcium and magnesium isotope systematics in rivers  
 985 draining the Himalaya-Tibetan-Plateau region: Lithological or fractionation control?  
 986 *Geochimica et Cosmochimica Acta*, 72(4): 1057-1075, doi:10.1016/j.gca.2007.11.029.  
 987 Tipper, E.T., Schmitt, A.-D., Gussone, N., 2016. Global Ca Cycles: Coupling of Continental and  
 988 Oceanic Processes, in Nikolaus Gussone et al., Calcium Stable Isotope Geochemistry.



Advances in Isotope Geochemistry, pp. 173-222.

Torres, M.A., West, A.J., Clark, K.E., 2015. Geomorphic regime modulates hydrologic control of chemical weathering in the Andes–Amazon. *Geochimica et Cosmochimica Acta*, 166: 105–128, doi:10.1016/j.gca.2015.06.007.

Walker, J.C.G., Hays, P.B., Kasting, J.F., 1981. A negative feedback mechanism for the long-term stabilization of Earth's surface temperature. *Journal of Geophysical Research*, 86(C10): 9776–9782, doi:10.1029/JC086iC10p09776.

Wang, S. et al., 2012. Calcium isotope fractionation and its controlling factors over authigenic carbonates in the cold seeps of the northern South China Sea. *Chinese Science Bulletin*, 57(11): 1325–1332, doi:10.1007/s11434-012-4990-9.

Wang, S. et al., 2013. Factors influencing methane-derived authigenic carbonate formation at cold seep from southwestern Dongsha area in the northern South China Sea. *Environmental Earth Sciences*, 71(5): 2087–2094, doi:10.1007/s12665-013-2611-9.

Wang, Y.-s., Chen, X.-x., Zhang, M.-n., 2018. Hydrochemistry and Chemical Weathering Processes of Malian River Basin. *Earth and Environment*, 46(1): 15–22 (*in Chinese with English abstract*).

Wellman, H., Wilson, A., 1965. Salt Weathering, a Neglected Geological Erosive Agent in Coastal and Arid Environments. *Nature*, 205(1097–1098), doi:10.1038/2051097a0.

West, A., Galy, A., Bickle, M., 2005. Tectonic and climatic controls on silicate weathering. *Earth and Planetary Science Letters*, 235(1–2): 211–228, doi:10.1016/j.epsl.2005.03.020.

White, A.F., Blum, A.E., 1995. Effects of climate on chemical weathering in watersheds. *Geochimica et Cosmochimica Acta*, 59(9): 1729–1747, doi:10.1016/0016-7037(95)00078-E.

Wiegand, B.A., Schwendenmann, L., 2013. Determination of Sr and Ca sources in small tropical catchments (La Selva, Costa Rica) – A comparison of Sr and Ca isotopes. *Journal of Hydrology*, 488: 110–117, doi:10.1016/j.jhydrol.2013.02.044.

Wu, W. et al., 2011. Mineralogy, major and trace element geochemistry of riverbed sediments in the headwaters of the Yangtze, Tongtian River and Jinsha River. *Journal of Asian Earth Sciences*, 40(2): 611–621, doi:10.1016/j.jseaes.2010.10.013.

Wu, W., Xu, S., Yang, J., Yin, H., Tao, X., 2009a. Sr fluxes and isotopic compositions in the headwaters of the Yangtze River, Tongtian River and Jinsha River originating from the Qinghai–Tibet Plateau. *Chemical Geology*, 260(1–2): 63–72, doi:10.1016/j.chemgeo.2008.12.007.

Wu, W. et al., 2009b. Sr fluxes and isotopic compositions of the eleven rivers originating from the Qinghai–Tibet Plateau and their contributions to  $^{87}\text{Sr}/^{86}\text{Sr}$  evolution of seawater. *Science in China Series D: Earth Sciences*, 52(8): 1059–1067, doi:10.1007/s11430-009-0084-1.

Wu, W., Yang, J., Xu, S., Yin, H., 2008. Geochemistry of the headwaters of the Yangtze River, Tongtian He and Jinsha Jiang: Silicate weathering and  $\text{CO}_2$  consumption. *Applied Geochemistry*, 23(12): 3712–3727, doi:10.1016/j.apgeochem.2008.09.005.

Wu, W., Zheng, H., Xu, S., Yang, J., Liu, W., 2013. Trace element geochemistry of riverbed and suspended sediments in the upper Yangtze River. *Journal of Geochemical Exploration*, 124: 67–78, doi:10.1016/j.gexplo.2012.08.005.

Xie, X., Li, H., Ju, Y., Chang, G., 2018. Analysis of Hydrological characteristics in Jinsha River Basin. *Sichuan Water Resources*, 6: 101–104 (*in Chinese with English abstract*).

Yu, S., Tang, Y., 1980. Hydrochemical characteristics of the saline lakes on the Qinghai–Xizang

1033 plateau, Proceedings of Symposium on Qinghai-Xizang (Tibet) Plateau, , Beijing, China.,  
1034 pp. 248.

1035 Zhang, L.-L. et al., 2016. Characteristics of water chemistry and its indication of chemical  
1036 weathering in Jinshajiang, Lancangjiang and Nujiang drainage basins. Environmental Earth  
1037 Sciences, 75(6), doi:10.1007/s12665-015-5115-y.

1038 Zhang, N., He, Y., Cao, J., Ho, K., Shen, Z., 2012. Long-term trends in chemical composition of  
1039 precipitation at Lijiang, southeast Tibetan Plateau, southwestern China. Atmospheric  
1040 Research, 106: 50-60, doi:10.1016/j.atmosres.2011.11.006.

1041 Zhang, X.-F., Yan, H.-c., Yao, Y., Lu, Y.-T., 2018. Analysis on the Sectional Annual Runoff Change  
1042 of the Jinsha River Basin in the Recent 50 Years. Resources and Environment in the Yangtze  
1043 Basin, 27(10): 2283-2292 (*in Chinese with English abstract*).

1044 Zhao, J.-C. et al., 2003. Origin of major elements and Sr isotope for river water in Yangtze River  
1045 source area. Hydrogeology & Engineering Geology(2): 89-93 (*in Chinese with English*  
1046 *abstract*).

1047 Zhao, T. et al., 2019. The influence of carbonate precipitation on riverine magnesium isotope  
1048 signals: new constrains from Jinsha River Basin, Southeast Tibetan Plateau. Geochimica et  
1049 Cosmochimica Acta, 248: 172-184, doi:10.1016/j.gca.2019.01.005.

1050 Zhong, J., 2017. Chemical weathering and carbon biogeochemical processes in the upper  
1051 Changjiang Basin impacted by the hydrological conditions, The University of Chinese  
1052 Academy of Sciences (*in Chinese with English abstract*).

1053 Zhu, P., Macdougall, J.D., 1988. Calcium isotopes in the marine environment and the oceanic  
1054 calcium cycle. Geochim Cosmochim Acta, 62(10): 1691-1698, doi:10.1016/S0016-  
1055 7037(98)00110-0.

1067

1068

1069

1070

1071

1072

1073

1074

**Table 1.** Chemical composition, Ca and Sr isotopic composition of the Jinsha River water.

Labels	Sample ID	T °C	pH	NDVI <sup>(a)</sup> %	Ca <sup>(b)</sup> μmol/L	Mg <sup>(b)</sup> μmol/L	Na <sup>(b)</sup> μmol/L	K <sup>(b)</sup> μmol/L	Si <sup>(b)</sup> μmol/L	Alk <sup>(b)</sup> μmol/L	SO <sub>4</sub> <sup>(b)</sup> μmol/L	Cl <sup>(b)</sup> μmol/L	NO <sub>3</sub> <sup>(b)</sup> μmol/L	Sr μmol/L	δ <sup>44/40</sup> Ca ‰	2sd	<sup>87</sup> Sr/ <sup>86</sup> Sr	2sd
Mainstream																		
JS-1	Mainstream	15.3	8.66	0.23	1341	878	5555	127	91	2973	1152	5183	30	9.35	1.11	0.14	0.7098	2.81E-05
JS-4	Mainstream	14.3	8.56	0.42	1213	759	4115	97	86	2847	923	3590	26	6.92	0.94	0.14	0.7101	2.73E-05
JS-7	Mainstream	16.8	8.47	0.46	920	463	1853	53	89	2162	520	1792	16	3.93	0.89	0.14	0.7107	2.61E-05
JS-10	Mainstream	17.9	8.46	0.47	861	418	1771	59	87	1273	481	1604	17	3.60	0.99	0.14	0.7106	2.34E-05
JS-12	Mainstream	18.2	8.43	--	803	372	1372	51	90	1772	398	1253	12	2.99	1.02	0.10	0.7108	3.50E-05
JS-15	Mainstream	16.6	8.42	--	770	347	1235	37	92	1064	358	1106	16	2.70	0.87	0.10	0.7108	2.31E-05
JS-20	Mainstream	21.4	8.35	0.53	920	447	1546	36	101	1956	443	1370	22	3.17	1.07	0.14	0.7105	2.80E-05
Tributaries																		
JS-2	Tongtian Rive	16.1	8.48	0.53	1134	580	252	20	72	2442	492	46	28	2.96	0.84	0.14	--	--
JS-3	Se Qu	16.5	8.28	0.51	957	585	165	26	83	2681	266	28	21	1.77	0.88	0.14	0.7142	2.51E-05
JS-5	Zhen Qu	14.8	8.32	0.73	530	219	98	15	95	1287	99	28	10	0.78	0.75	0.10	0.7144	2.72E-05
JS-6	Ba Qu	12.7	8.25	0.42	755	288	112	30	88	2002	339	6	6	1.48	0.78	0.14	0.7157	2.32E-05
JS-8	Zong Qu	16.9	8.17	0.49	600	175	109	24	97	1412	54	12	15	0.76	0.83	0.14	0.7130	2.11E-05
JS-9	Ding Qu	14.4	8.23	0.46	538	158	81	32	93	1902	72	10	5	0.81	0.68	0.14	0.7126	2.31E-05
JS-11	Gang Qu	15.7	8.44	0.61	827	257	96	16	82	1751	172	12	5	2.27	0.75	0.10	0.7090	2.31E-05
JS-13	Zhubaluo Rive	15.1	8.41	0.63	469	72	41	7	71	940	48	7	3	0.64	0.81	0.14	0.7118	2.48E-05
JS-14	Chongjiang Ri	15.5	8.23	0.60	453	117	47	21	107	1695	15	12	14	0.81	0.74	0.14	0.7102	2.75E-05
JS-16	Shuoduogang	12.8	8.14	0.56	712	230	80	10	84	1719	42	9	4	1.11	0.87	0.14	0.7091	2.31E-05
JS-18	Renli River	22.4	8.06	0.56	920	400	195	39	113	2304	101	75	43	1.19	0.83	0.14	0.7108	2.98E-05
Gypsum																		
G1-1	near Dang Qu														0.27	0.10		
G1-2	near Dang Qu														0.24	0.10		
G2	near Tuotuohe														0.80	0.10		
G3-1	near Tuotuohe														0.80	0.10		
G3-2	near Tuotuohe														0.95	0.10		

1075

1076 (a) NDVI: The Normalized Difference Vegetation Index calculated by GIS. (b) Major element data from Zhong (2017).

1077

1078

1079

1080 **Table 2.** Saturation Index of carbonates and clay minerals in the Jinsha River.

River labels	Mineral types						
	Calcite	Dolomite	Illite	Chlorite	Montmorillonite	Kalinite	Kmica
	Saturation index of minerals (SI)						
Mainstream							
JS-1	0.93	1.67	-0.39	3.60	2.96	1.32	4.98
JS-4	0.79	1.35	-0.29	2.34	2.86	1.60	5.18
JS-7	0.56	0.84	-0.28	1.58	2.69	1.83	5.21
JS-10	0.32	0.36	-0.34	1.59	2.67	1.77	5.19
JS-12	0.42	0.54	-0.04	1.48	2.89	2.09	5.88
JS-15	0.16	-0.01	0.10	1.02	2.89	2.29	5.71
JS-20	0.47	0.72	-0.83	1.40	2.71	1.47	4.47
Tributaries							
JS-2	0.71	1.14	-1.94	0.76	1.49	0.68	3.07
JS-3	0.51	0.82	-0.62	0.24	2.29	1.88	4.80
JS-5	0.01	-0.38	-0.24	-1.27	2.38	2.33	5.24
JS-6	0.22	-0.03	0.93	-1.26	2.94	3.28	6.86
JS-8	-0.01	-0.54	0.20	-2.20	2.70	2.73	5.95
JS-9	0.08	-0.38	1.74	-1.36	3.56	4.00	7.98
JS-11	0.44	0.37	-0.40	0.16	2.35	2.11	5.08
JS-13	0.07	-0.96	-0.73	-2.84	1.80	2.21	4.84
JS-14	-0.01	-0.60	0.60	-2.51	2.88	3.05	6.40
JS-16	0.05	-0.44	0.52	-2.68	2.64	3.30	6.33
JS-18	0.32	0.37	-0.01	-0.31	3.13	2.38	5.60

1081

1082

1083

1084

1085

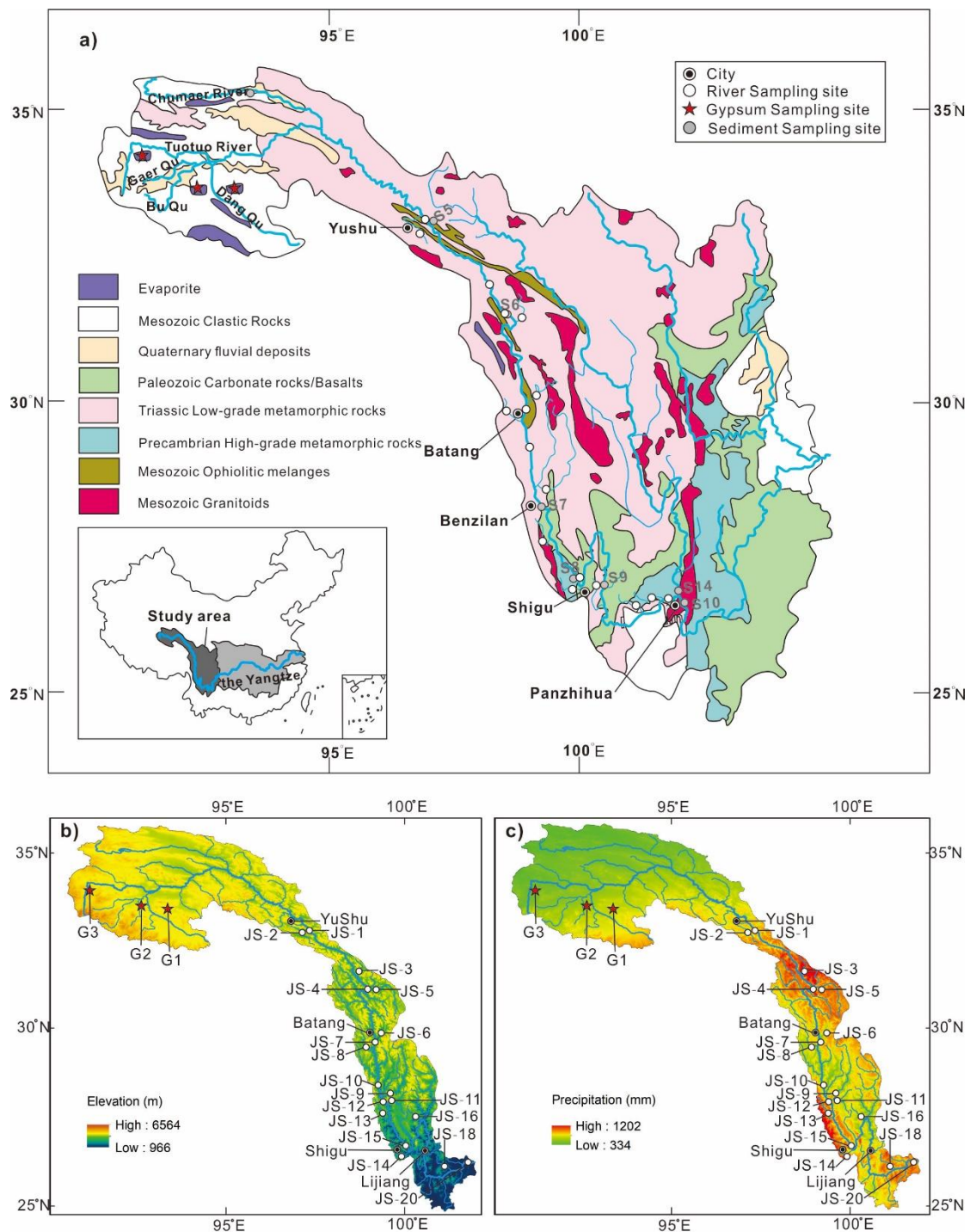
1086

1087

1088

**Table 3.** The fractionation factor and the amount of Ca precipitation in the Jinsha River water.

River labels	Equilibrium fractionation model					
	$\alpha = 0.99935$		$\alpha = 0.99953$		$\alpha = 0.99963$	
	$f_{Ca}$	Removed Ca(%)	$f_{Ca}$	Removed Ca(%)	$f_{Ca}$	Removed Ca(%)
Mainstream						
JS-1	0.07	93	0.07	93	0.07	93
JS-4	0.16	84	0.16	84	0.16	84
JS-7	0.27	73	0.27	73	0.27	73
JS-10	0.26	74	0.26	74	0.26	74
JS-12	0.32	68	0.32	68	0.32	68
JS-15	0.34	66	0.34	66	0.34	66
JS-20	0.32	68	0.32	68	0.32	68
Tributaries						
JS-2	0.68	32	0.55	45	0.43	57
JS-3	0.62	38	0.47	53	0.32	68
JS-5	0.82	18	0.75	25	0.69	31
JS-6	0.77	23	0.68	32	0.59	41
JS-8	0.70	30	0.58	42	0.47	53
JS-9	0.92	8	0.90	10	0.87	13
JS-11	0.82	18	0.75	25	0.68	32
JS-13	0.72	28	0.62	38	0.51	49
JS-14	0.83	17	0.76	24	0.70	30
JS-16	0.63	37	0.49	51	0.35	65
JS-18	0.69	31	0.57	43	0.46	54



1100  
1101 **Fig. 1.** (a) Geological map of the headwaters of the Changjiang River and the  
1102 Jinsha River basin, modified from (Wu et al., 2011); (b) and (c) show elevation  
1103 and precipitation of the Jinsha River basin separately. White solid circles  
1104 represent the river sampling site of this study, grey solid circles (S5-S14) are

sediment sampling locations in previous research (Wu et al., 2011), red stars represent gypsum sampling sites and the concentric circles are cities.

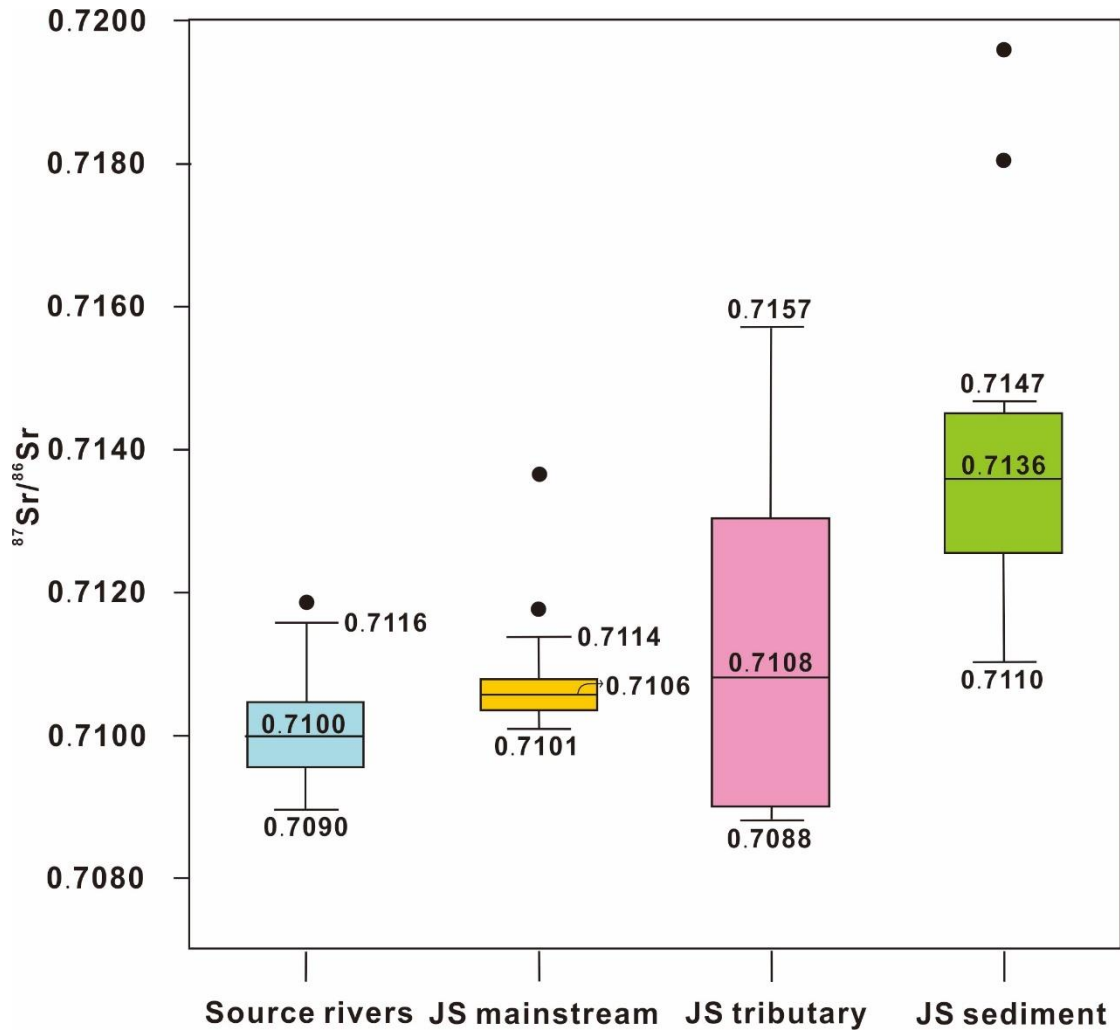


**Fig. 2.** Sr isotopic compositions in the Jinsha River basin. Each box consists of a rectangle and three horizontal lines. Those horizontal lines represent the min value, median value and max value of the data separately from bottom to upper. The bottom horizontal line of the rectangle represents the first quartile (25%), which is the median of the data points lower than the median. And median is the second quartile. On the contrary, the top horizontal line represents the third quartile (75%), which is the median of the data points



higher than the median. The black dots mean abnormal values.

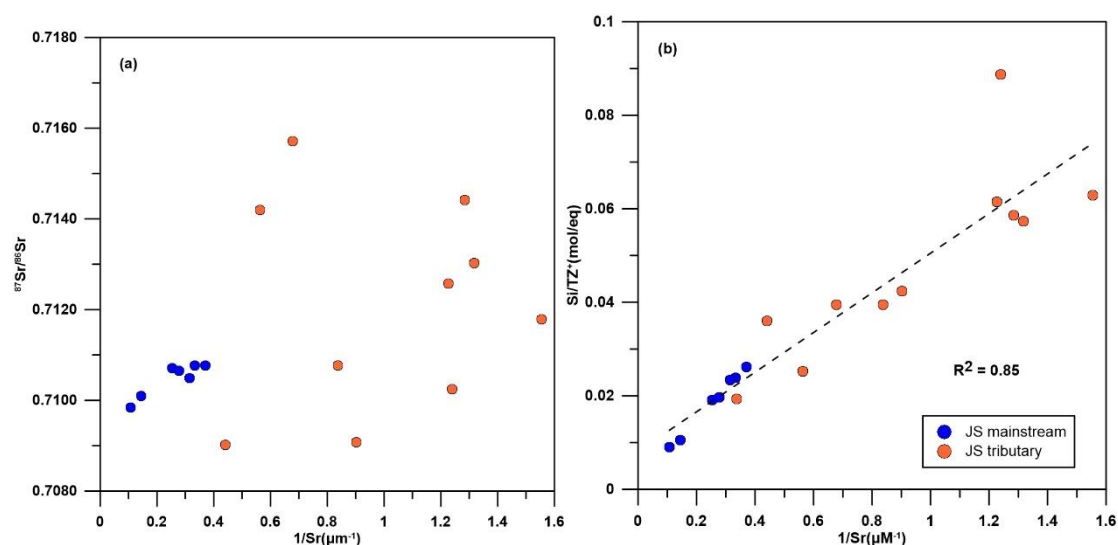


**Fig. 3.** (a) A plot of  $1/Sr$  and  $^{87}Sr/^{86}Sr$  in the Jinsha River; (b) A plot of  $1/Sr$  and  $Si/TZ^+$  in the Jinsha River.

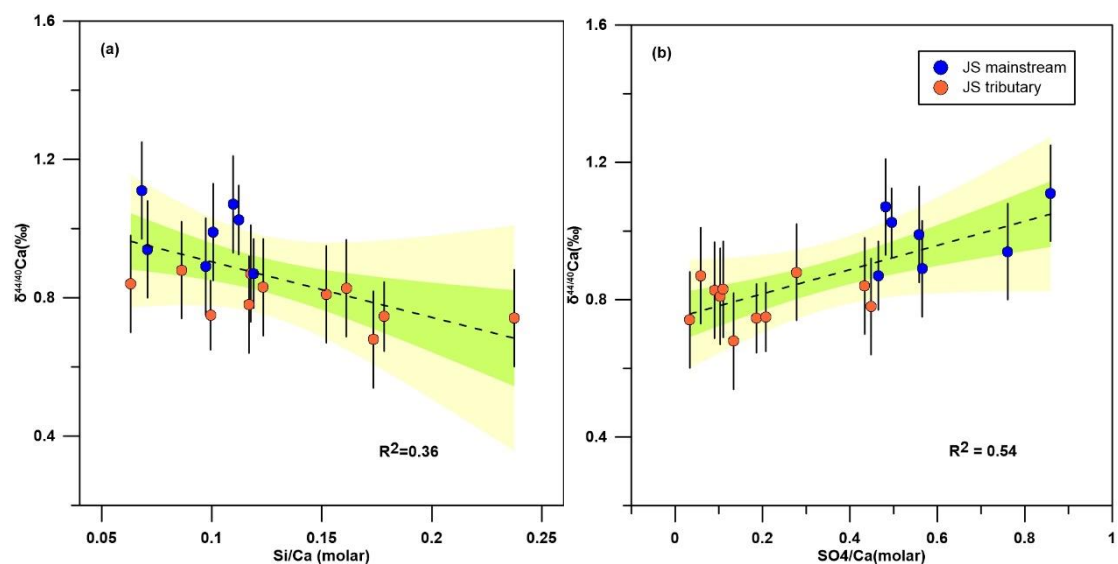


**Fig. 4.** (a) Plot of  $Si/Ca$  and  $\delta^{44/40}Ca$  in the Jinsha River; (b) Plot of  $SO_4/Ca$  and  $\delta^{44/40}Ca$  in the Jinsha River. The green and yellow areas represent 95% and 99.99% confidence interval, respectively.

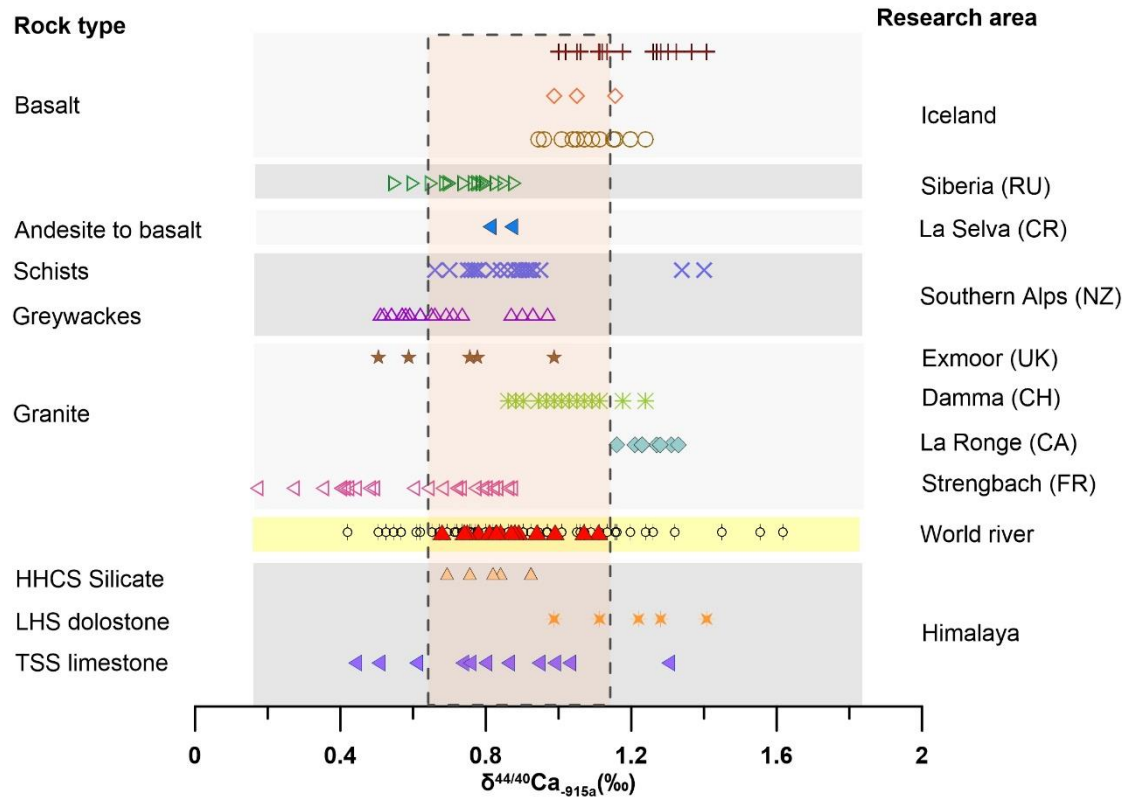


**Fig. 5.** Ca isotopic variation in river waters (modified from (Schmitt, 2016)). The red solid triangles represent our data in this study; world river data are from (Schmitt et al., 2003; Tipper et al., 2006; Tipper et al., 2010; Zhu and Macdougall, 1988) and other data sources can be seen in text. All values are normalized to the NIST SMR 915a standard.

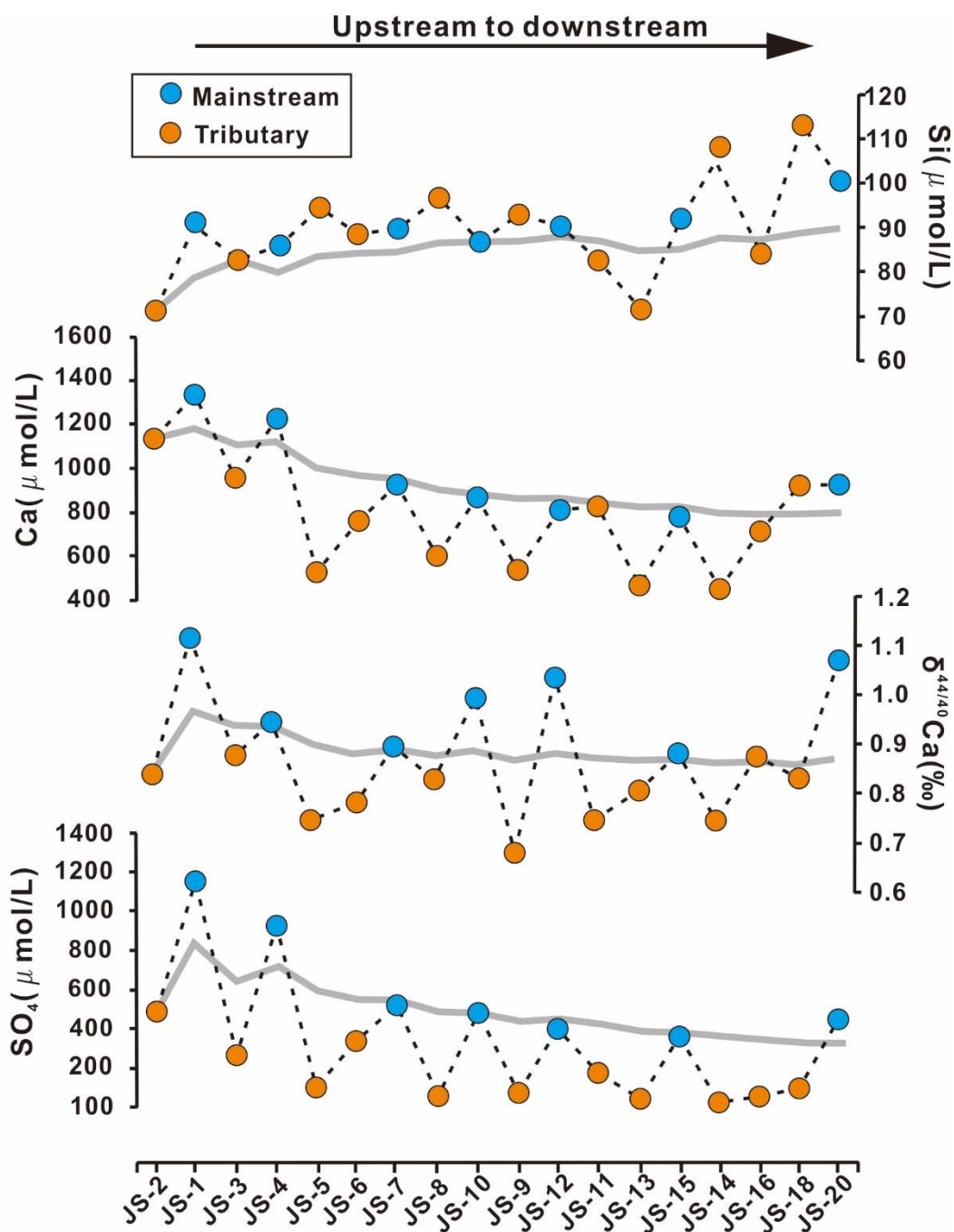


**Fig. 6.** Si, Ca and  $\text{SO}_4$  concentrations and Ca isotope compositions of the Jinsha River water samples from upstream to downstream. Grey lines represent moving averages of all of the corresponding data.

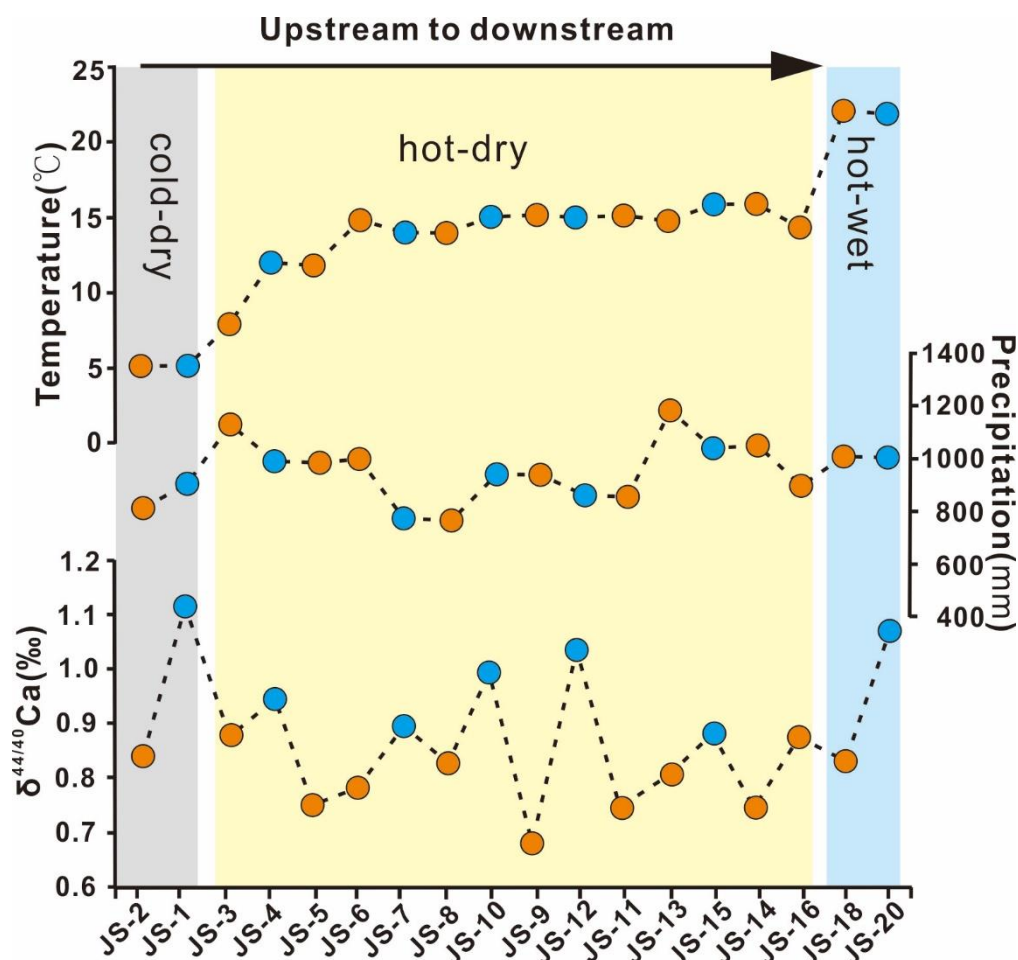


**Fig. 7.** The change of climate factors (air temperature and precipitation) and Ca isotope compositions of the Jinsha River water samples from upstream to downstream. The Grey rectangle area represents the dry-cold climate, the yellow area represents the dry and hot environments and the blue area represents the hot-wet climate.

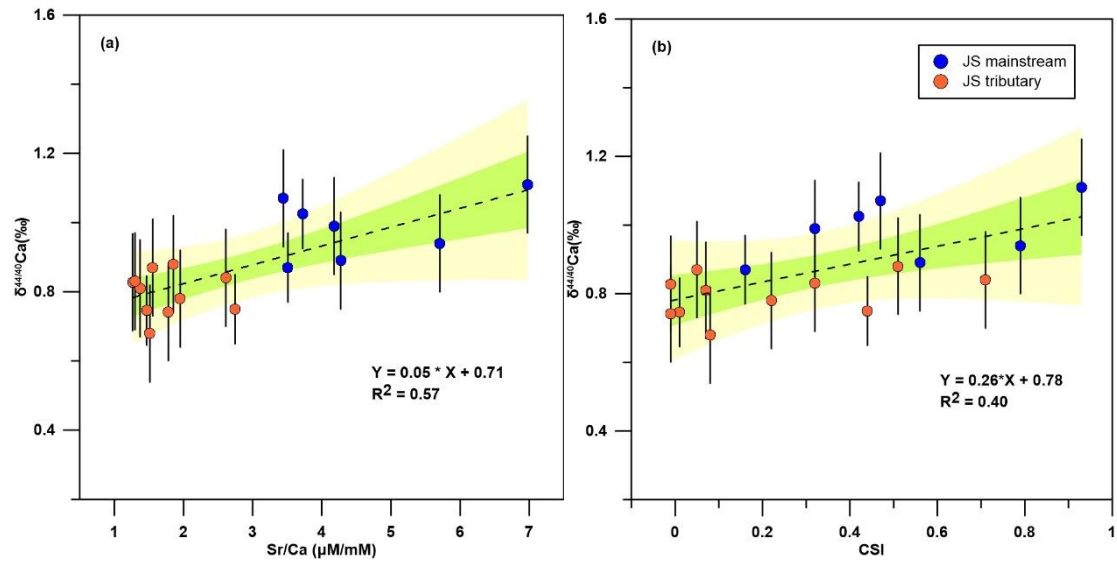


**Fig. 8.** (a) A plot of Sr/Ca and  $\delta^{44/40}\text{Ca}$  in the Jinsha River; (b) A plot of CSI and  $\delta^{44/40}\text{Ca}$  in the Jinsha River. The green and yellow area represents the 95% and 99.99% confidence interval respectively.

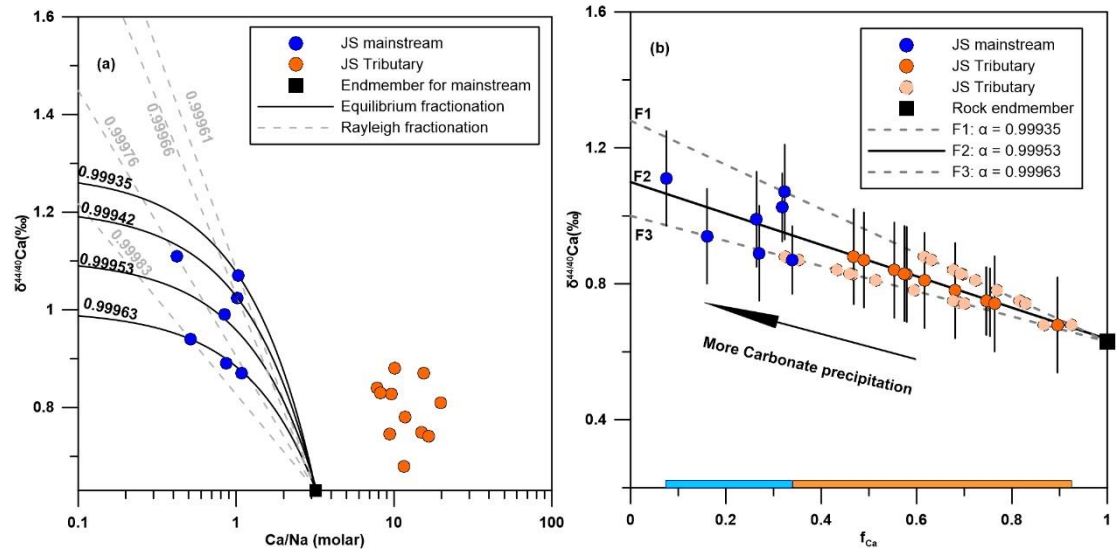


**Fig. 9.** The relationships between Ca isotope composition of river waters and (a) dissolved Ca/Na ratios and (b) the fraction of Ca remaining in solution ( $f_{\text{Ca}}$ ) under the Equilibrium model.